MIXED L1/H∞-SYNTHESIS FOR L∞-STABILITY

Pierre Apkarian, Dominikus Noll

MIXED L_1/H_∞-SYNTHESIS FOR L_∞-STABILITY

PIERRE APKARIAN[1] AND DOMINIKUS NOLL[2]

ABSTRACT. We consider stabilization and performance optimization of non-linear controlled systems, where the non-linearity satisfies a sector constraint asymptotically. This leads to optimization of the closed loop peak-to-peak system norm subject to H_∞-performance constraints. Non-linear controlled systems tuned successfully by this novel approach are locally exponentially stable and globally BIBO-stable.

KEY WORDS. BIBO-stability · peak-to-peak norm · asymptotic constraint · boundary feedback control · wave equation · sector non-linearity

1. INTRODUCTION

The peak-gain, or peak-to-peak norm of a BIBO-stable linear time-invariant system G, is the time-domain L_∞ operator norm,

$$\|G\|_{\text{pk\_gn}} = \sup\{|G * w|_\infty : |w|_\infty \leq 1\}, \tag{1}$$

where the signal norm on $L_\infty([0,\infty),\mathbb{R}^n)$ is $|x|_\infty = \sup_{t\geq 0} \max_{i=1,\ldots,n} |x_i(t)|$. In the SISO case it is also known as the system L_1-norm. As opposed to the more standard H_2- or H_∞-norms, computation or optimization of $\|G\|_{\text{pk\_gn}}$ has found only mild attention in the control literature, even though its importance e.g. for the rejection of persistent perturbations was recognized [27, 28, 29, 34, 41, 54, 65]. One of the reasons of this disesteem is probably the link of $\|\cdot\|_{\text{pk\_gn}}$ with the H_∞-norm $\|\cdot\|_\infty$, where in the chain

$$m^{-1/2}\|G\|_\infty \leq \|G\|_{\text{pk\_gn}} \leq (2n+1)p^{1/2}\|G\|_\infty \tag{2}$$

the right-hand estimate holds for real-rational systems G with n poles and p inputs, while the left-hand estimate is valid even for infinite dimensional well-posed BIBO-stable systems with m outputs. This may have been interpreted in the sense that optimizing $\|G\|_{\text{pk\_gn}}$ offers nothing substantial over optimizing $\|G\|_\infty$. In the present work we show that optimizing $\|G\|_{\text{pk\_gn}}$ has genuine scope.

For the purpose of motivation, we consider a possibly infinite-dimensional Lur'e system, where a tunable LTI (Linear Time-Invariant) block is in loop with a sector non-linearity. By the Small Gain theorem closed-loop L_2-stability is assured if one succeeds in tuning the LTI-block to satisfy a suitable H_∞-norm or frequency shape constraint. However, this sufficient conditions may be difficult, or even impossible, to achieve if the sector is too large. Here our new approach applies and replaces the large sector by a smaller one, which the non-linearity satisfies only asymptotically. Application of a small gain argument now requires working with the time-domain L_∞-norm instead of the L_2-norm. In consequence, the LTI-block is now tuned to satisfy a constraint in the peak-to-peak norm (1). If successful, the non-linear closed loop is BIBO stable. Due to the smaller primal sector, this is often easier to achieve than the original H_∞-constraint, and it is one of the few remaining options for non-linear systems with different attraction regimes.

[1]ONERA, Department of System Dynamics, Toulouse, France.
[2]Institut de Mathématiques, Université de Toulouse, France.

This approach via *asymptotic sectors* may be combined with H_∞-methods to guarantee local exponential stability along with global BIBO-stability. This leads to a novel type of mixed peak-gain/H_∞-optimization program.

In order to demonstrate the potential of our method, we discuss feedback control of a wave equation with a non-linear anti-damping boundary causing instability. This model has been used to control slipstick vibrations in drilling systems [19, 23, 55, 56, 57]. Our method allows to prove local exponential stability in tandem with global BIBO-stability for scenarios, where this was previously impossible, the challenge being to achieve this with finite-dimensional controllers of simple implementable structure. The second part of the paper extends the concept of asymptotic constraints to MIMO non-linearities, highlighting that applications are not limited to the SISO case.

The organization is as follows. In Section 2 we discuss the case of a sector non-linearity. An algorithm based on mixed H_∞/H_∞- and peak-gain/H_∞-programs is presented in Section 2.2. In Section 2.3 we show how the aperture of the asymptotic sector may be optimized, a feature which is not possible with standard sectors. Section 3 discusses the application to the control of slipstick vibrations. Section 4 resumes theory and extends the asymptotic concept to MIMO non-linearity along with illustrations and applications. Properties of the peak-to-peak norm and implementation of the mixed programs are discussed in Section 5.

2. Mixed program for a Lur'e systems

For the purpose of motivation we consider a controlled Lur'e system with state x, control input u, measured output y, disturbances w, and regulated outputs z:

$$G_{nl}: \quad \begin{aligned} \dot{x} &= Ax + B_p p + B_w w + B_u u \\ q &= C_q x \qquad\qquad + D_q u \\ p &= \phi(t,q) \\ z &= C_z x \qquad + D_{zw} w + D_{zu} u \\ y &= C_y x \end{aligned} \tag{3}$$

where $p(t) = \phi(t, q(t))$ is a non-linearity satisfying $\phi(t,0) = 0$, $\frac{\partial \phi}{\partial q}(t,0) = 0$ and a sector constraint

$$(\phi(t,q) - aq) \cdot (\phi(t,q) - bq) \leq 0$$

for all $t \geq 0$ and all q, abbreviated $\phi \in \mathbf{sect}(a,b)$. Since $a \leq \frac{\partial \phi}{\partial q}(t,0) = 0 \leq b$, the linearized system is

$$G: \quad \begin{aligned} \dot{x} &= Ax + B_w w + B_u u \\ z &= C_z x + D_{zw} w + D_{zu} u \\ y &= C_y x \end{aligned} \tag{4}$$

In nominal H_∞-synthesis, we might interpret the non-linearity as a mere disturbance and optimize a suitable closed-loop performance channel $\|T_{zw}(G,K)\|_\infty$ over a class $K \in \mathscr{K}$ of structured controllers [7], with optimal H_∞-controller $K^* \in \mathscr{K}$ and gain $\gamma_\infty = \|T_{zw}(G,K^*)\|_\infty$.

Suppose this optimistic approach of representing the non-linearity by a disturbance w (as in Fig. 2 right) is too unspecific and K^* is not entirely satisfactory. Then we have to target the sector non-linearity explicitly (as in Fig. 2 left). Putting $c = (b+a)/2$, $r = (b-a)/2$, and $\psi(t,q) = \phi(t,q) - cq$, we have $\psi \in \mathbf{sect}(-r,r)$. The non-linear system

(3) is now equivalently written as

$$G_{nl}: \quad \begin{aligned} \dot{x} &= Ax + cB_pC_qx + B_pp + B_uu \\ q &= C_qx \qquad\qquad + D_qu \\ p &= \psi(t,q) \\ y &= C_yx \end{aligned} \tag{5}$$

where the performance channel $w \to z$ is temporarily ignored for notational convenience. We introduce $A_\psi = A + cB_pC_q$ and

$$G_\psi: \quad \begin{aligned} \dot{x} &= A_\psi x + B_pp + B_uu \\ q &= C_qx \qquad + D_qu \\ y &= C_yx \end{aligned} \tag{6}$$

then (3) is equivalent to putting $p \to q$ of G_ψ in loop with the centered non-linearity $\psi(\cdot) = \phi(\cdot) - cI$.

Closing the controller loop $u = Ky$ in G_ψ leads to the channel $q = T_{qp}(G_\psi, K)p$. Suppose now we succeed in tuning $K^\sharp \in \mathscr{K}$ such that $(G_\psi, K^\sharp)$ is L_2-stable and satisfies the estimate $\|T_{qp}(G_\psi, K^\sharp)\|_\infty < r^{-1}$. Then by the small-gain theorem the non-linear loop $(T_{qp}(G_\psi, K^\sharp), \psi)$ is L_2-stable, hence so is $(G_{nl}, K^\sharp)$. This is addressed by the structured mixed H_∞/H_∞-optimization program

$$\begin{array}{ll} \text{minimize} & \|T_{qp}(G_\psi, K)\|_\infty \\ \text{subject to} & \|T_{wz}(G, K)\|_\infty \le (1+\tau)\gamma_\infty \\ & K \text{ stabilizes } G, G_\psi \\ & K \in \mathscr{K} \end{array} \tag{7}$$

which optimizes stability of the non-linear system G_{nl} under a constraint allowing a controlled loss of performance in the linearized channel $w \to z$, where $K \in \mathscr{K}$ ranges over a class of structured controllers in the sense of [7]. This is also known as multi-disk optimization [8]. The algorithmic solution proposed in that reference is implemented in the `systune` package of [72], which we use to solve (7) algorithmically.

Proposition 1. *Suppose the solution $K^\sharp \in \mathscr{K}$ of (7) satisfies $\|T_{qp}(G_\psi, K^\sharp)\|_\infty < r^{-1}$. Then the loop $(G_{\rm nl}, K^\sharp)$ is stable in the L_2-sense. That is, for every $w \in L_2[0,\infty)$ and every x_0 the solution of the non-homogenous Cauchy problem $\dot{x}_{cl} = A_{cl}(K^\sharp)x_{cl} + B_p\phi(C_qx) + B_ww$, $x_{cl}(0) = x_0$ is in $L_2[0,\infty)$. Moreover $\gamma_\infty^\sharp = \|T_{zw}(G, K^\sharp)\|_\infty \le (1+\tau)\gamma_\infty$.* □

Remark 1. Note that (G, K) and (G_ψ, K) have different closed loop system matrices. The A-matrix of G is A, that of G_ψ is A_ψ, so we have a structured simultaneous stabilization problem, which is known to be NP-hard for most structures.

2.1. **Asymptotic sector constraint.** Apart from the fact that optimization in (7) is over structured controllers $K \in \mathscr{K}$, the method so far is standard. The situation changes if the sector $\mathbf{sect}(a,b)$ is too large, so that tuning K to achieve $\|T_{qp}(G_\psi, K)\|_\infty < r^{-1}$ fails. Then we have to change strategy! What we propose in this work is to choose a different sector, also noted $\mathbf{sect}(a,b)$ for simplicity, which the non-linearity ϕ now satisfies only asymptotically, where Fig. 1 shows schematically what we have in mind.

Definition 1. (Asymptotic sector). A non-linearity $p = \phi(t,q)$ satisfies a sector constraint asymptotically, noted $\phi \sim \mathbf{sect}(a,b)$, if there exist $M, L > 0$ such that for every $t \ge 0$, $(\phi(t,q) - aq)(\phi(t,q) - bq) \le 0$ for $|p| > M$, and $|\phi(t,q)| \le L$ for $|q| \le M$.

Suppose we have identified a new typically smaller sector with $\phi \sim \mathbf{sect}(a,b)$. (See for instance Fig. 1 for some basic examples of asymptotic sector constraints). We center

the non-linearity, now with the new $c = (b+a)/2, r = (b-a)/2$, which leads to a new $\psi(t,p) = \phi(t,p) - cp$, now satisfying the sector constraint $\psi \sim \mathbf{sect}(-r,r)$ asymptotically. With G_ψ taken with regard to the new ψ, the non-linearity (3) is still equivalent to this modified loop (G_ψ, ψ). Now we consider the mixed `peak-gain`/H_∞-optimization program

$$\begin{array}{ll} \text{minimize} & \|T_{pq}(G_\psi, K)\|_{\text{pk\_gn}} \\ \text{subject to} & \|T_{wz}(G,K)\|_\infty \le (1+\tau)\gamma_\infty \\ & K \text{ stabilizes } G, G_\psi \\ & K \in \mathscr{K} \end{array} \tag{8}$$

where $T_{qp}(G_\psi, K)$ is the channel $p \to q$ of the modified G_ψ in feedback with K. This optimizes the peak-gain norm of $p \to q$ subject to a controlled loss of H_∞-performance in the channel $w \to z$ over the optimistic performance γ_∞ achieved by $K^* \in \mathscr{K}$. The algorithmic solution of this novel mixed synthesis program will be discussed in Section 5.2.

We now have the following consequence of the Small-Gain theorem (compare [42, 66]), see also Theorem 3:

Theorem 1. *Let $K^\flat \in \mathscr{K}$ be a solution of program (8) satisfying $\|T_{pq}(G_\psi, K^\flat)\|_{\text{pk\_gn}} < r^{-1}$. Then for every input $w \in L_\infty[0,\infty)$ and all initial conditions x_0 the non-linear closed loop $\dot{x}_{cl} = A_{cl}(K^\flat)x_{cl} + B_p\phi(C_q x) + B_w w$ has trajectories in $(L_\infty[0,\infty), |\cdot|_\infty)$, and is locally exponentially stable.* □

2.2. **Algorithm.** The findings of the previous sections lead to the following strategy:

Algorithm: Mixed peak-gain/H_∞-control of Lur'e system G_{nl}

1: **Steady-state.** Compute steady state of non-linear system G_{nl}, shift it to origin, and obtain linearization G.

2: **Nominal synthesis.** Fix performance and robustness specifications and perform nominal synthesis for G, interpreting non-linearity as a disturbance. Optimal K^* gives lower bound $\gamma_\infty = \|T_{wz}(G,K^*)\|_\infty$.

3: **Sector.** Using $\phi \in \mathbf{sect}(a_0, b_0)$, let $c_0 = (b_0+a_0)/2$, $r_0 = (b_0-a_0)/2$, form $\psi_0 = \phi - c_0 I$, and represent non-linear system G_{nl} as loop (G_{ψ_0}, ψ_0).

4: **Complementary sector.** Attempt closed-loop L_2-stability by solving

$$\begin{array}{ll} \text{minimize} & \|T_{qp}(G_{\psi_0}, K)\|_\infty \\ \text{subject to} & \|T_{wz}(G,K)\|_\infty \le (1+\tau)\gamma_\infty \\ & K \in \mathscr{K} \end{array}$$

If optimal solution $K^\sharp \in \mathscr{K}$ satisfies $\|T_{pq}(G_{\psi_0}, K^\sharp)\|_\infty < r_0^{-1}$, quit successfully. Otherwise continue with step 5.

5: **Asymptotic sector.** Find asymptotic sector $\phi \sim \mathbf{sect}(a,b)$. Form $c = (b+a)/2$, $r = (b-a)/2$, and $\psi = \phi - cI$. Represent G_{nl} as loop (G_ψ, ψ).

6: **Complementary asymptotic sector.** Attempt closed-loop BIBO-stability in tandem with local exponential stability by solving

$$\begin{array}{ll} \text{minimize} & \|T_{qp}(G_\psi, K)\|_{\text{pk\_gn}} \\ \text{subject to} & \|T_{wz}(G,K)\|_\infty \le (1+\tau)\gamma_\infty \\ & K \in \mathscr{K} \end{array}$$

If optimal solution $K^\flat$ satisfies $\|T_{qp}(G_\psi, K^\flat)\|_{\text{pk\_gn}} < r^{-1}$ quit successfully.

Remark 2. By (2) we have $\|G\|_\infty \le \|G\|_{\text{pk\_gn}}$ even for infinite dimensional systems, so that $\|T_{pq}(G_\psi, K)\|_{\text{pk\_gn}} < 1$ implies $\|T_{pq}(G_\psi, K)\|_\infty < 1$. Therefore it makes no sense to

choose the asymptotic sector as a true sector. We need $\phi \sim \mathbf{sect}(a,b)$, but must have $\phi \notin \mathbf{sect}(a,b)$, as $\phi \in \mathbf{sect}(a,b)$ would mean trying step 4 again, saddled with the even harder constraint $\|T_{pq}(G_\psi, K)\|_{\mathrm{pk\_gn}} < 1$.

2.3. **Best asymptotic sector.** Working with asymptotic sectors offers additional flexibility over conventional sectors, which we now exploit. Consider step 6 of the algorithm. Instead of choosing the asymptotic sector $\mathbf{sect}(a,b)$, which is the same as choosing c, r, we could in the first place only choose c. With $\psi(t,q) = \phi(t,q) - cq$, we solve program

$$(8') \qquad \begin{array}{ll} \text{minimize} & \|T_{pq}(G_{\phi-c}, K)\|_{\mathrm{pk\_gn}} \\ \text{subject to} & \|T_{wz}(G,K)\|_\infty \le (1+\tau)\gamma_\infty \\ & K \in \mathscr{K} \end{array}$$

where r is not yet determined. The optimal controller $K(c) \in \mathscr{K}$ now depends on c, and as in step 6 of the algorithm, provides the value

$$(9) \qquad r(c) := 1/\|T_{pq}(G_{\phi-c}, K(c))\|_{\mathrm{pk\_gn}}.$$

This gives a curve $r = r(c)$, and on putting $a = c - r(c)$, $b = c + r(c)$, it remains to check whether $\mathbf{sect}(a,b)$ is an asymptotic sector for ϕ.

An interesting case is when ϕ has a slope at infinity, i.e., when $\lim_{|x|\to\infty} \frac{\phi(t,x)}{x} = q_\infty$ exists independently of t. Then every choice $a < q_\infty < b$ gives $\phi \sim \mathbf{sect}(a,b)$, so with (9) we have to check whether

$$(10) \qquad c - r(c) < q_\infty < c + r(c).$$

As soon as this holds, we have *a posteriori* found an asymptotic sector $\phi \sim \mathbf{sect}(a,b)$ as $a = c - r(c)$ and $b = c + r(c)$. We can then also determine the parameters L, M in the definition of an asymptotic sector. The smaller M, the closer the asymptotic sector comes to a true sector.

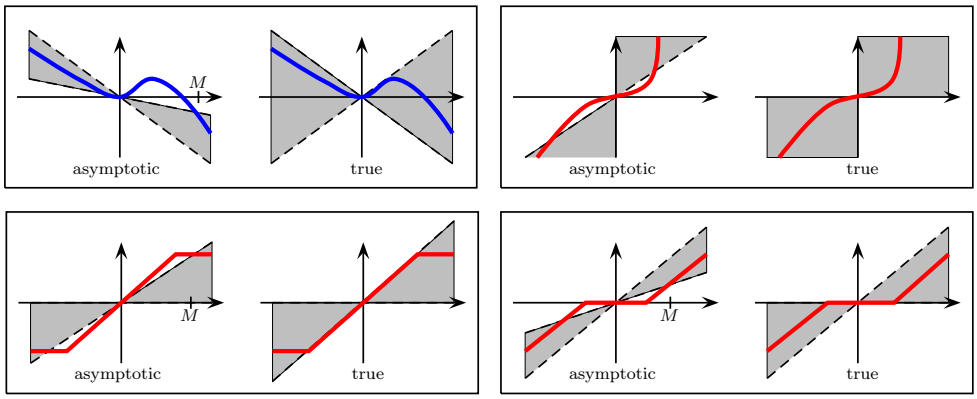

FIGURE 1. Schematic view of true and asymptotic sectors for general sector non-linearity (upper left), positivity (upper right), saturation (lower left), and dead time (lower right). Asymptotic sector constraints are satisfied for large values $|q| > M$.

Since the asymptotic sector is chosen in response to failure of the true sector $\mathbf{sect}(a_0, b_0)$, we typically initialize the search for a, b by values c close to q_∞, as this increases the chances of program (8′) to succeed. This highlights why an asymptotic sector typically will not satisfy $0 \in [a,b]$, whereas this is always satisfied for the true sector.

Remark 3. For every c the aperture $2r(c)$ of the candidate sector is maximized through program (8) due to (9). Over the range of those c where (10) holds, the resulting curve

$(c, r(c))$ serves as a Pareto optimal front, from which we will pick our ultimate c. The decision will not just be based on the size of the aperture of $\mathbf{sect}(a, b)$, it may also matter how close $\mathbf{sect}(a, b)$ is to a true sector, how large the constant $k = LM$ is, and ultimately, how $G_{\rm nl}$ in loop with $K(c)$ behaves in non-linear simulations. This method will be applied to the slipstick study in Section 3.

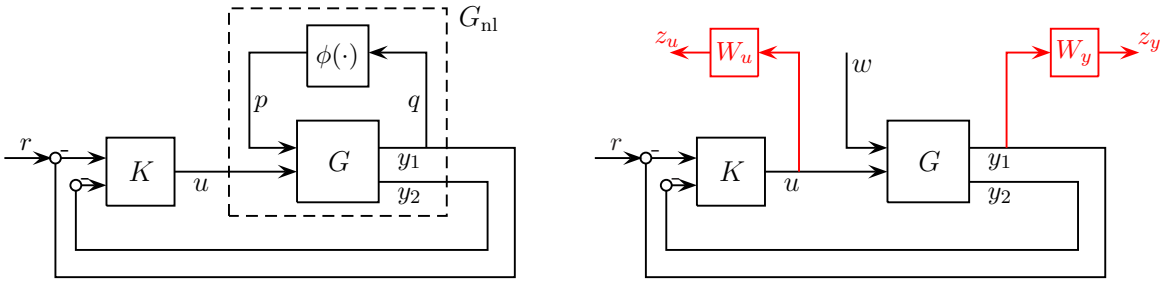

FIGURE 2. Lur'e system $G_{\rm nl}$ as loop between non-linearity ϕ and LTI system G (left). Nominal H_∞-synthesis with G and non-linearity interpreted as disturbance w (right).

3. Application: BIBO-stable control of slipstick vibrations

We consider control of a damped wave equation with instability caused by non-linear boundary anti-damping dynamics,

$$G_{\rm nl}: \quad \begin{aligned} x_{tt}(\xi,t) &= x_{\xi\xi}(\xi,t) - 2\lambda x_t(\xi,t), \quad 0<\xi<1, t\geq 0 \\ x_\xi(1,t) &= -x_t(1,t) + u(t) \\ \alpha x_{tt}(0,t) &= x_\xi(0,t) + q x_t(0,t) + \phi(x_t(0,t)) \end{aligned} \tag{11}$$

where (x, x_t) is the state, $u(t)$ the boundary control, and the measured outputs are

$$y_1(t) = x_t(0,t), \quad y_2(t) = x_t(1,t). \tag{12}$$

The non-linearity satisfies $\phi(0) = 0$, $\phi'(0) = 0$, so that the linearized system G in (4) is obtained by dropping the term $\phi(x_t)$. System $G_{\rm nl}$ has among others been used to model slipstick vibrations in drilling systems, see [4] and the references given there. The challenge is to control $G_{\rm nl}$ with a finite-dimensional controller $u = Ky$ of simple, implementable structure such that slipstick caused by the non-linear boundary friction term $\phi(x_t)$ can be avoided or at least mitigated.

In these applications $\lambda \geq 0$, $\alpha \geq 0$, $q \geq 0$ are typically positive, and the non-linearity derives from a frictional force depending on the angular velocity of the drill

$$T(\omega) = \gamma_1\omega + \left(\gamma_2 + \gamma_3 e^{-\gamma_4|\omega|}\right)\operatorname{sign}(\omega),$$

exhibiting a sharp jump at $\omega = 0$, which based on experimental evidence in comparable situations [52], is slightly mollified around 0. With $\bar\omega > 0$, the nominal angular speed of the drill, step 1 of the algorithm leads to the centered non-linearity

$$\phi(\omega) = T(\bar\omega) - T(\bar\omega + \omega) + T'(\bar\omega)\cdot\omega$$

as in (3), shown in Fig. 3 for two of the scenarios studied in [4]. This corresponds to step 1 of the algorithm.

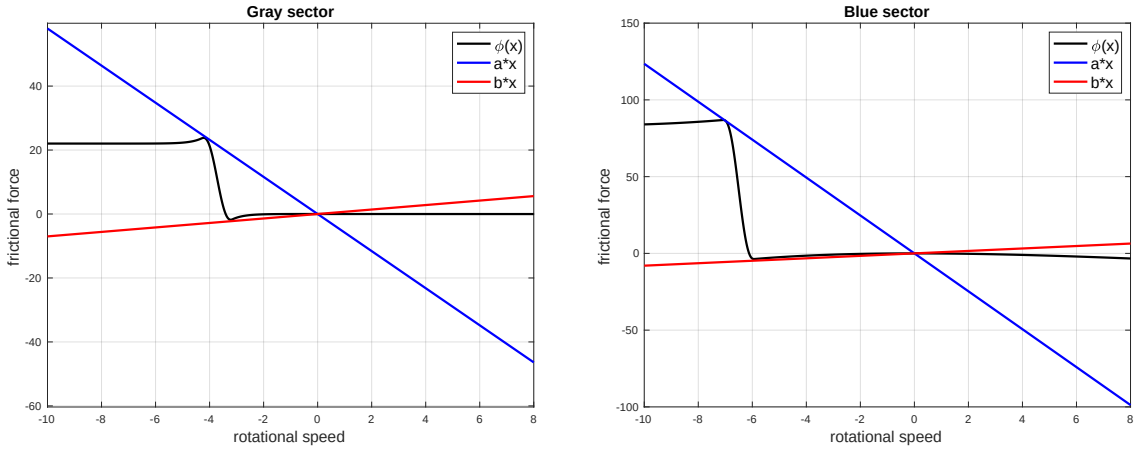

FIGURE 3. Sector non-linearity ϕ in slipstick model with strong jump at $-\overline{\omega}$ for two scenarios labeled 'gray' and 'blue' in [4].

We continue to follow the pattern of the algorithm. By [4, sect. 3-4] the number of unstable open-loop poles of G is $n_p(q,\alpha,\lambda) \in \{0,1,2\}$, and several scenarios 'gray', 'blue', 'red', 'magenta' and 'green' were analyzed. The blue scenario, on which we focus here, has two unstable open-loop poles, the numerical parameters gathered in Table 1. Here the aperture of the sector $\mathbf{sect}(a_0,b_0)$ in Fig. 3 (right) is extremely large, and step 4 of the algorithm fails even when a rather conservative τ is chosen. This is where we use the asymptotic sector of step 5 of the algorithm.

Numerical values for slipstick study

	q	α	λ	$\overline{\omega}$	γ_1	γ_2	γ_3	γ_4
gray	0.0019	0.7994	0.1957	3.7186	1.002e-4	11.0034	6.6020	2.4203
blue	0.9797	0.1828	0.5477	6.5044	1.002e-4	28.8697	17.3218	0.1537

TABLE 1

From [4, Lemma 4] we know that $\phi(\omega)$ behaves asymptotically as $\phi(\omega) \sim a_\pm + \phi'(\infty)\omega$ for $\omega \to \pm\infty$ with $\phi'(\infty) = -0.9797$. This means, every choice $a < \phi'(\infty) < b$ gives rise to an asymptotic sector $\phi \sim \mathbf{sect}(a,b)$. This can for instance be seen in Fig. 6. We now have to give the details of step 6 of the algorithm.

As in Fig. 2 (right), we consider a nominal linear model, where the non-linearity is interpreted as a disturbance w. We optimize the closed-loop H_∞-channel $T_{(r,w)\to(z_u,z_y)}(G,K)$, where a high pass filter W_u is used for the control signal, and a low-pass for tracking of output y_1, which corresponds to the rotational speed at the drill bit. The rationale is that attenuating the disturbance w should reduce the effect of the non-linearity. This leads to the nominal H_∞-performance $\gamma_\infty = \|T_{(r,w)\to(z_u,z_y)}(G,K_\infty)\|_\infty$ for an H_∞-controller $K_\infty \in \mathscr{K}$. As proved in [4], exponential stabilizability and detectability of the linear open loop guarantee that the linear closed loop $T_{(r,w)\to(z_u,z_y)}(G,K_\infty)$ is not only H_∞-stable, but even exponentially stable, and as a consequence, BIBO-stable.

Since it is necessary to consider asymptotic sectors, we choose the parameter c, and obtain the loop transformed system $G_{\phi-c}$. This corresponds to representing the non-linearity as a feedback loop as in Fig. 2 (left), and we now have to optimize the peak gain norm of the closed-loop channel $p \to q$ in $G_{\phi-c}$. This is the mixed peak-gain/H_∞

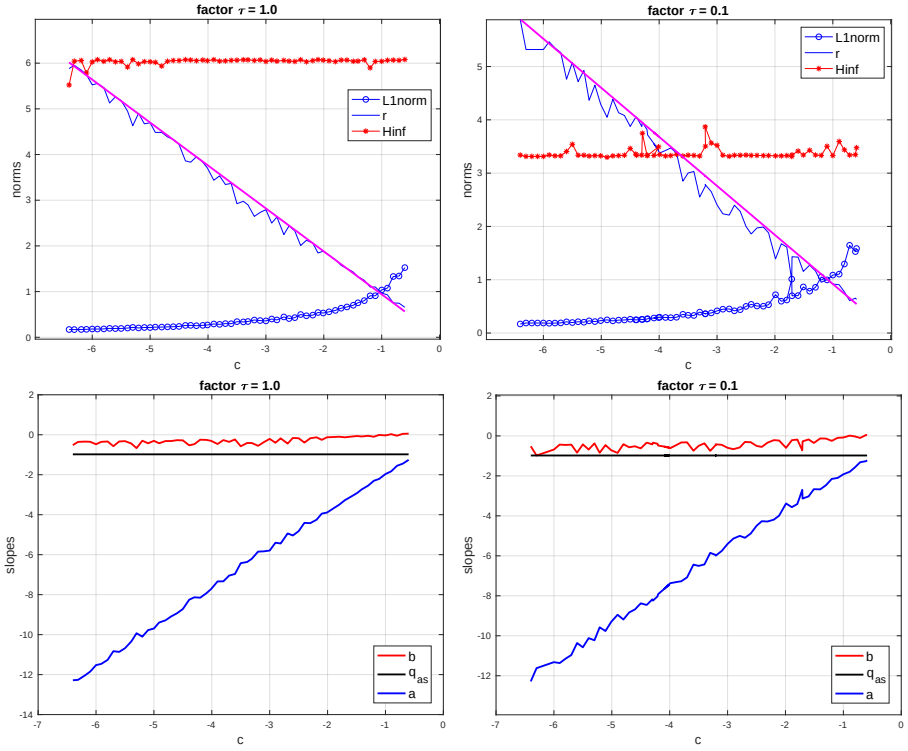

FIGURE 4. Program (13) was run for $c \in [-6.2, -0.5]$ and $\tau = 0.1$ (right), $\tau = 1.0$ (left). Upper row shows best achieved $1/r(c)$ as $-\mathrm{o}-$, with $r(c) \approx -0.94 \cdot c$ shown as — for $\tau = 1.0$ and -0.92 for $\tau = 0.1$, depending essentially linearly on c (magenta). Nominal H_∞-norm is 3.03, and $-*-$ shows result after optimization. Lower row shows slopes a (blue), b (red) of asymptotic sectors with $a < q_{as} < b$ and $b = c + r(c)$, $a = c - r(c)$.

program

$$
\begin{array}{ll}
\text{minimize} & \|T_{qp}(G_{\phi-c}, K)\|_{\text{pk\_gn}} \\
\text{subject to} & \|T_{(r,w)\to(z_u,z_y)}(G, K)\|_\infty \le (1+\tau)\gamma_\infty \\
& K \text{ stabilizes } G, G_{\phi-c} \\
& K \in \mathscr{K}
\end{array} \tag{13}
$$

which leads to the optimal $K_{\text{opt}}(c) \in \mathscr{K}$ with value $1/r(c) = \|T_{qp}(G_{\phi-c}, K_{\text{opt}}(c))\|_{\text{pk\_gn}}$. Then we compute $a = c - r(c)$, $b = c + r(c)$, and if $a < q_\infty < b$, then the non-linearity is asymptotically in the sector, so that the non-linear closed loop is BIBO-stable. In our experiment $\mathscr{K}$ designates 3rd order controllers, which due to $n_y = 2$, $n_p = 1$ leads to 18 optimization variables. Fig. 4 shows these curves for two scenarios $\tau = 0.1$ and $\tau = 1.0$, with c in the range $c \in [-6.2, -0.5]$.

Remark 4. Application of our theory requires some preparation, as the system is now infinite dimensional and of boundary control type. We have to clarify the meaning of the impulse response $ce^{A_{cl}t}b$ representing the closed-loop channel $w \to z$. Following [26, Sect. 3.3], [4, sect. 5], the linear wave equation and boundary feedback controller can after a change of variables be represented as an abstract boundary control system

$$
\begin{aligned}
&\dot{x} = \mathscr{A}x, \ \ \mathscr{P}x = u + w \\
&y = \mathscr{C}x, \ \ z = \mathscr{C}_1 x \\
&u = Ky
\end{aligned}
$$

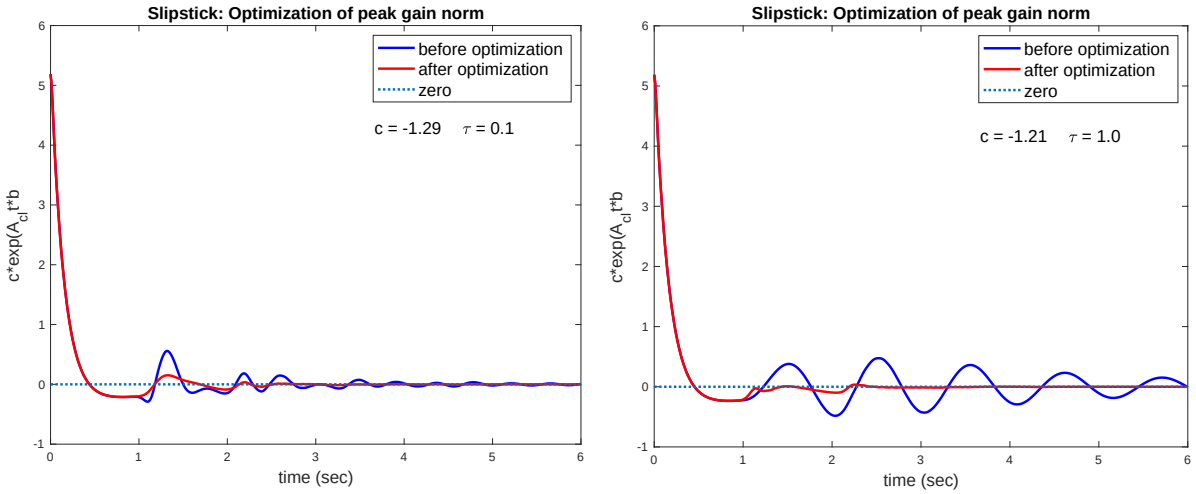

FIGURE 5. Impulse response before and after optimization (8) for two cases $c = -1.29$, $\tau = 0.1$ and $c = -1.21$, $\tau = 1.0$.

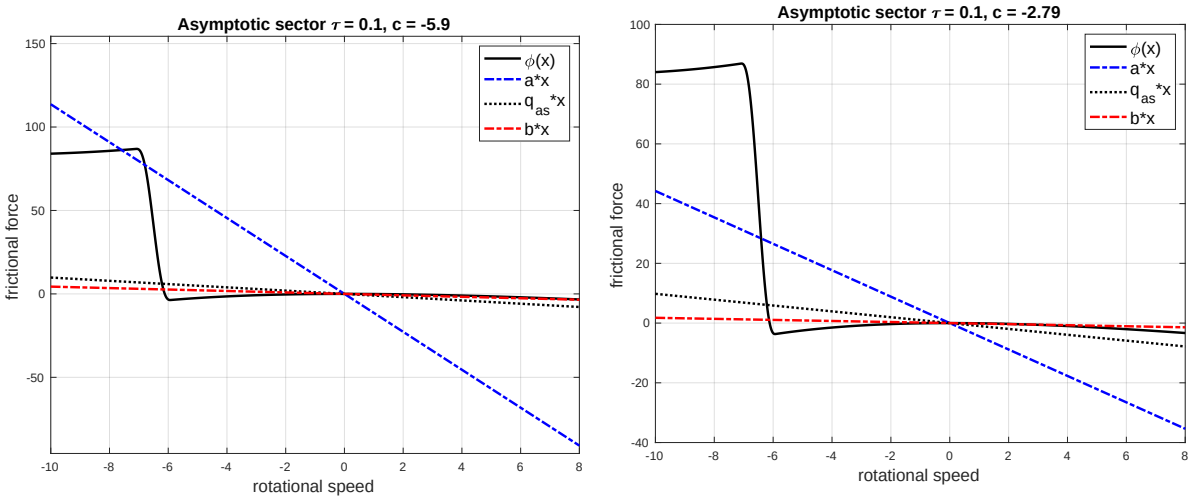

FIGURE 6. Asymptotic sectors for $\tau = 0.1$ and $c = -5.9$, $c = -2.79$, with $r(c)$ computed via (13). Constraints are satisfied for large angular velocities.

where $u = Ky$ is a finite-dimensional controller, and where $\mathscr{A} : D(\mathscr{A}) \to Z$, Z a separable Hilbert space, $u(t) \in \mathbb{R}^p$, $\mathscr{P} : D(\mathscr{P}) \to \mathbb{R}^p$, $D(\mathscr{A}) \subset D(\mathscr{P}) \subset Z$, $D(A) = D(\mathscr{A}) \cap \ker(\mathscr{P})$ is dense and $A = \mathscr{A}|D(A)$ generates a C_0-semi-group on Z. Moreover, there exists a bounded operator $B \in L(\mathbb{R}^p, Z)$ such that $Bu \in D(\mathscr{A})$ for every u, $\mathscr{A}B \in L(\mathbb{R}^p, Z)$, and $\mathscr{P}Bu = u$ for every u. In [4, Thm. 2] the case $w = 0$ was handled, and in order to accommodate the Lur'e non-linearity, we have to make a slight extension. As [4, Thm. 2] shows, a finite-dimensional H_∞-stabilizing controller with minimal representation renders the closed loop in this state-space representation exponentially stable. That means the channel $w \to z$ is represented as $ce^{A_{cl}t}b$, where $b(\xi)w \in D(A_{cl})$ and A_{cl} generates an exponentially stable semi-group. Hence $e^{A_{cl}t}b$ is a classical solution, and since A_{cl} is exponentially stable, $e^{A_{cl}t}b \in L^1$ by the Datko-Pazy theorem [36, Thm. V.1.8]. This implies $ce^{A_{cl}t}b \in L^1$. In consequence, the impulse response is convenient to optimize, even though we expect a singularity at $t = 0$ (see e.g. Fig 5).

Remark 5. We recall that for linear systems BIBO-stability implies H_∞-stability, and for finite-dimensional LTI-systems the two are equivalent. There exist infinite dimensional

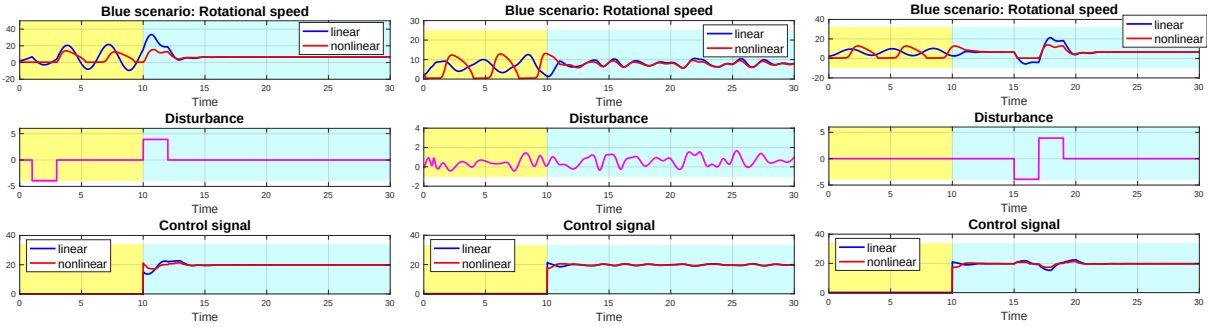

FIGURE 7. $c = -5.21$, $\tau = 0.1$. Initial value below steady state, causing slipstick. Controller switched on at $t = 10$. Uncontrolled system shows slipstick.

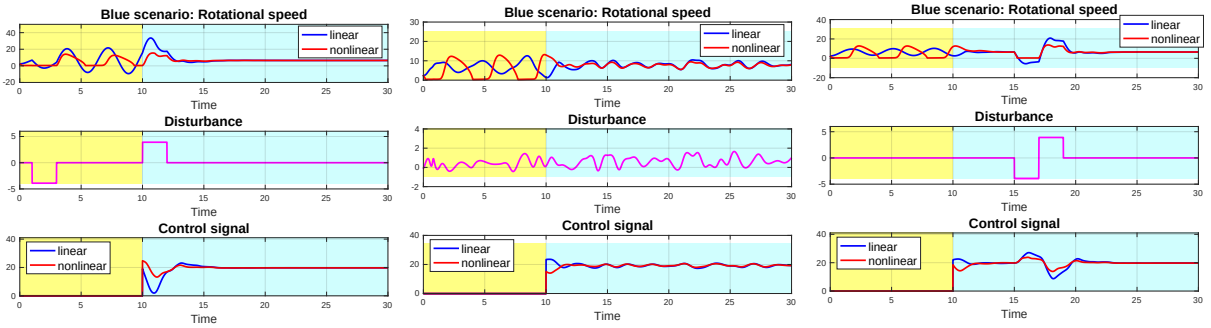

FIGURE 8. $c = -2.79$, $\tau = 0.1$. Initial value below steady state, causing slipstick. Controller switched on at $t = 10$. Three types of disturbances. Controller manages to free system from slipstick.

LTI-systems which are H_∞-stable, but not BIBO stable. However, if the system is H_∞-stable and exponentially stabilizable and detectable, then it is exponential stable [25], and that implies BIBO stability. The latter because if the growth rate of A is < 0, then there exists $a > 0$ such that $|ce^{At}b| \leq Me^{-at}$, which implies integrability of $ce^{At}b$.

Results. Experiments with different tolerances $\tau = 1.0$ and $\tau = 0.1$ were performed. In each case the parameter c varied in the interval $[-6.2, -0.5]$ and optimization led to an asymptotic sector, see Fig. 4. Smaller values of c lead to larger aperture in the sectors. Two scenarios were selected and underwent non-linear simulations with three types of disturbances shown in Figs. 7 and 8. The resulting asymptotic sectors are shown in Fig. 6, and typical optimized impulse responses are shown in Fig. 5.

4. Extension to multi-dimensional non-linearity

In order to extend our algorithm to systems (3) with multi-dimensional non-linearity, we consider a feedback loop between an LTI-system G and the non-linearity Δ:

$$\begin{aligned} v &= Gw + f \\ w &= \Delta(v) + e \end{aligned} \tag{14}$$

as shown in Fig. 9 (left). Well posedness of (14) in the L_2-sense means that G, Δ are L_2-bounded causal operators on L_{2e}, and that the map $(v, w) \to (e, f)$ has a causal inverse on L_{2e}. The system is L_2-stable if this inverse is bounded, i.e., if there exists a constant $c > 0$ with

$$|v|_2^2 + |w|_2^2 \leq c\left(|f|_2^2 + |e|_2^2\right)$$

for any solution of (14). Since we are interested in BIBO-stability, we also need the corresponding notions in the time-domain L_∞-sense.

Definition 2. The feedback connection (G, Δ) is well-posed in the time-domain L_∞ sense if Δ and G both map $L_{\infty e}$ into $L_{\infty e}$, and if the map $(v, w) \to (e, f)$ from (14) has a causal inverse $(e, f) \to (v, w)$ on the spaces $L_{\infty e} \times L_{\infty e} \to L_{\infty e} \times L_{\infty e}$.

Definition 3. The L_∞-well-posed feedback connection (G, Δ) is BIBO-stable, if in the setting of (14) there exist constants $k_1 > 0$, $k_2 > 0$, such that

$$|v|_\infty + |w|_\infty \leq k_1 \left(|e|_\infty + |f|_\infty\right) + k_2$$

for all $e, f \in L_\infty([0, \infty), \mathbb{R}^n)$.

We now investigate ways in which the steps of the algorithm in Section 2.2 may be extended to MIMO non-linearity (14).

4.1. **Extending the mixed H_∞/H_∞-program.** Extending step 4 to MIMO non-linearity leads to Integral Quadratic Constraints (IQC), where Δ and G in loop as in (14) satisfy the quadratic constraints induced by a multiplier $\Pi = \Pi^\sim$:

$$\left\langle \begin{bmatrix} u \\ \Delta(u) \end{bmatrix}, \Pi \begin{bmatrix} u \\ \Delta(u) \end{bmatrix} \right\rangle_T \leq 0, \quad \left\langle \begin{bmatrix} Gu \\ u \end{bmatrix}, \Pi \begin{bmatrix} Gu \\ u \end{bmatrix} \right\rangle_T \geq 0 \tag{15}$$

for every $u \in L_{2e}$ and every $T \geq 0$. While [44] assures L_2-stability of the loop if one of the inequalities is satisfied strictly, the crucial question is how the IQC for G may be verified algorithmically. In the literature these are traditionally transformed to LMIs, but in synthesis lead to BMIs, which are known to encounter numerical difficulties. This was recognized in [9, 10, 1], where non-differentiable optimization techniques in tandem with Hamiltonian tests for function evaluations [16] were preferred instead. Recently this line has been further perfected in [22, 69].

In [69], the authors obtain a mixed H_∞/H_∞-program expanding on (8) for J-spectral factorable multipliers $\Pi(s) = \Psi^\sim(s) J \Psi(s)$, where $J = [I_p, 0; 0, -I_m]$ and $\Psi(s)$ is a L_2-bistable rational system. Defining processes

$$\begin{bmatrix} \Psi_{11}u + \Psi_{12}\Delta(u) \\ \Psi_{21}u + \Psi_{22}\Delta(u) \end{bmatrix} =: \begin{bmatrix} \widetilde{u} \\ \widetilde{\Delta}(\widetilde{u}) \end{bmatrix}, \quad \begin{bmatrix} \Psi_{11}Gu + \Psi_{12}u \\ \Psi_{21}Gu + \Psi_{22}u \end{bmatrix} =: \begin{bmatrix} \widetilde{G}\widetilde{u} \\ \widetilde{u} \end{bmatrix}, \tag{16}$$

L_2-stability of the loop (G, Δ) is equivalent to L_2-stability of the loop $(\widetilde{G}, \widetilde{\Delta})$. Assuming that Δ is square, it follows from [69, Thm. 5] that $\widetilde{G} = (\Psi_{11}G + \Psi_{12})(\Psi_{21}G + \Psi_{22})^{-1}$ is well-posed, and the IQC for G in (15) is transformed into $\|\widetilde{G}\|_\infty \leq 1$. Similarly, with $\circ$ denoting map or relation composition, $\widetilde{\Delta} = (\Psi_{22}\Delta + \Psi_{21}) \circ (\Psi_{12}\Delta + \Psi_{11})^{-1}$, and due to (15), left, this process is an L_2 contraction, i.e., signals $z_1 = \Psi_{11}u + \Psi_{12}\Delta(u)$ and $z_2 = \Psi_{21}u + \Psi_{22}\Delta(u)$ satisfy $\int_0^T |z_2(t)|^2 dt \leq \int_0^T |z_1(t)|^2 dt$ for all $T > 0$. What is not clear is whether $\widetilde{\Delta}$ is a mapping.

We now present an alternative way to obtain a mixed H_∞/H_∞-program, which gives an explicit loop transformation and, as we shall see, is also applicable to positivity type factorizations. Consider again IQC multipliers $\Pi(s)$ factored as

$$\Pi(j\omega) = \Psi(j\omega)^* P \Psi(j\omega) \tag{17}$$

for a bistable LTI-system $\Psi(s)$ and a static invertible $P = P^T$. Such factorizations exist for rational $\Pi = \Pi^\sim$ if Π has neither poles nor zeros on $j\mathbb{R}$ and allows no equalizing vectors, i.e., no $u \in \mathscr{H}_2$, $u \neq 0$, with $\Pi u \in \mathscr{H}_2^\perp$; cf. [45]. In particular, positive-negative multipliers satisfying $\Pi_{11}(j\omega) \succeq \epsilon I$ and $\Pi_{22}(j\omega) \preceq -\epsilon I$ for some $\epsilon > 0$ admit such factorizations [58]. Following [59, Thm. 6], there is no harm in assuming that both

IQCs in (15) are satisfied strictly. Now define a new augmented interconnection (G_a, Δ_a) as

$$G_a = \Psi \begin{bmatrix} -I & 2G \\ 0 & I \end{bmatrix} \Psi^{-1}, \quad \Delta_a = \Psi \circ \begin{bmatrix} I & 0 \\ 2\Delta & -I \end{bmatrix} \circ \Psi^{-1}, \tag{18}$$

then by [68, Thm. 2 (1)], L_2-stability of (G, Δ) is equivalent to L_2-stability of (G_a, Δ_a).

Adopting $\Pi_{11} \succeq \epsilon I$ and $\Pi_{22} \preceq -\epsilon I$ for some $\epsilon > 0$, it follows from [68, Thm. 2 (2)] that Δ_a, G_a satisfy IQCs for the passivity multiplier $P_a = [0, P; P, 0]$ strictly, i.e.,

$$\begin{aligned} \int_0^T p_a(t)^T G_a(P^{-1}p_a)(t)dt &\le -\epsilon \int_0^T p_a(t)^T p_a(t)dt \\ \int_0^T p_a(t)^T P\Delta_a(p_a)(t)dt &\ge \epsilon \int_0^T p_a(t)^T p_a(t)dt \end{aligned} \tag{19}$$

for some $\epsilon > 0$ and every $T \ge 0$, where $p_a = (p, q)^T$.

The inequalities in (19) are now turned into bounded gain conditions using Möbius or bilinear transformations. We introduce

$$G_e := \mathcal{B} \star G_a P^{-1} = (G_a P^{-1} - I)^{-1}(G_a P^{-1} + I) \tag{20}$$

and

$$\Delta_e = P \circ \Delta_a \star \mathcal{B} = (I + P \circ \Delta_a)^{-1} \circ (I - P \circ \Delta_a) \tag{21}$$

with

$$\mathcal{B} := \begin{bmatrix} -I & \sqrt{2}I \\ -\sqrt{2}I & I \end{bmatrix},$$

where $\star$ is the Redheffer star product [53]. Here $(I + P\Delta_a)^{-1}$ and $(G_a P^{-1} - I)^{-1}$ are well-defined and stable due to (19) and the passivity theorem, hence Δ_e, G_e are well-defined and L_2-stable. Indeed, $(I + P \circ \Delta_a)^{-1}$ is the negative feedback loop between the upper block I and the lower block $P \circ \Delta_a$. Since $P \circ \Delta_a$ is strictly passive by (19) and I is passive, stability follows from the passivity theorem [70]. A similar argument applies to $(G_a P^{-1} - I)^{-1}$. Owing to $\mathcal{B} \star \mathcal{B} = I^\sharp = [0, I; I, 0]$, the unit of the star product, we get (stability) loop invariance $(G_a, \Delta_a) \cong (G_a P^{-1}, P \circ \Delta_a) \cong (\mathcal{B} \star G_a P^{-1}, P \circ \Delta_a \star \mathcal{B}) = (G_e, \Delta_e)$. This means the passivity-type conditions (19) are equivalent to bounded-gain conditions

$$\begin{aligned} \int_0^T \|G_e(p_e)(t)\|^2 dt &\le (1 - \epsilon) \int_0^T \|p_e(t)\|^2 dt \\ \int_0^T \|\Delta_e(p_e)(t)\|^2 dt &\le (1 - \epsilon) \int_0^T \|p_e(t)\|^2 dt\,, \end{aligned} \tag{22}$$

for some $\epsilon > 0$ and every $T \ge 0$, where $p_e = (p, q)^T$. See [33, pp. 215-16] for a proof, which also applies to the non-linear case.

From $\Delta_e = P \circ \Delta_a \star \mathcal{B}$ we have $\Delta_e \star \mathcal{B} = P \circ \Delta_a \star \mathcal{B} \star \mathcal{B} = P \circ \Delta_a \star I^\sharp = P \circ \Delta_a$, hence $\Delta_a = P^{-1} \circ \Delta_e \star \mathcal{B}$. That gives $\begin{bmatrix} I & 0 \\ 2\Delta & -I \end{bmatrix} = \Psi^{-1} P^{-1} \circ \Delta_e \star \mathcal{B}\Psi$. Hence,

$$\Delta = \begin{bmatrix} \frac{I}{\sqrt{2}} \\ \frac{I}{\sqrt{2}} \end{bmatrix}^T \Psi^{-1}(P^{-1} \circ \Delta_e \star \mathcal{B})\Psi \begin{bmatrix} \frac{I}{\sqrt{2}} \\ \frac{I}{\sqrt{2}} \end{bmatrix}, \tag{23}$$

which gives the inverse operation to $\Delta \to \Delta_e$ in (21). What we have obtained is a parametrization of all non-linearities Δ derived from L_2-contractions Δ_e via the loop transformation through $\Psi(s), P$, or equivalently, all non-linearities satisfying IQCs with factorable multiplies $\Pi = \Psi^* P \Psi$. For these Δ the IQC-stability theorem can now be reduced to the small gain theorem [70].

Theorem 2. (IQC as H_∞ constraint). *Suppose (G,Δ) is loop transformed to (G_e,Δ_e), where Δ satisfies the IQC with multiplier $\Pi=\Psi^*P\Psi$ factored with bistable $\Psi(s)$ and invertible $P=P^T$. Then $\|G_e\|_\infty<1$ implies L_2-stability of the loop (G,Δ).* □

Applying the loop transformation $(G,\Delta)\cong(G_e,\Delta_e)$ to the closed loop system $\mathcal{F}_l(G,K)$ leads to $(\mathcal{F}_l(G,K),\Delta)\cong(\mathcal{F}_l(G,K)_e,\Delta_e)$. This allows us now to extend step 4 of the algorithm to IQCs.

Corollary 1. *Suppose the mixed H_∞/H_∞-synthesis program*

$$\begin{array}{ll}\text{minimize} & \|\mathcal{F}_l(G,K)_e\|_\infty \\ \text{subject to} & \|T_{wz}(G,K)\|_\infty\le(1+\tau)\gamma_\infty \\ & K\in\mathscr{K}\end{array} \tag{24}$$

admits an optimal solution $K^\sharp\in\mathscr{K}$ satisfying $\|\mathcal{F}_l(G,K^\sharp)_e\|_\infty<1$. Then $K^\sharp$ stabilizes the loop (G,Δ) in the L_2-sense, and linearized closed loop performance is degraded over nominal performance γ_∞ by no more than the factor $1+\tau$. □

Remark 6. Program (24) is now a natural MIMO-extension of (7). It can be efficiently solved by the method of [7, 8] available in the `systune` package of [72, 2, 8]. This is numerically preferable to transforming IQCs to BMIs. With the recent extension of non-smooth H_∞-synthesis in [6, 5, 4] it becomes even possible to address (24) for infinite-dimensional systems with infinite-dimensional multipliers $\Psi(s)$.

Remark 7. An advantage of this construction is that when (G,Δ) satisfies an IQC with positivity multiplier as in (19), then going from (G,Δ) to (G_a,Δ_a) can be skipped and we build (G_e,Δ_e) directly without the augmentation (18).

For multipliers $\Pi(s)$ with a lower triangular factorizations both approaches (16) and the augmentation $G\to G_a\to G_e$ lead to the same result. Suppose

$$\Pi(j\omega)=\Psi^T(-j\omega)P\Psi(j\omega),\quad \Psi=\begin{bmatrix}\Psi_{11}&0\\ \Psi_{21}&\Psi_{22}\end{bmatrix}\quad P=\begin{bmatrix}I&0\\0&-I\end{bmatrix}, \tag{25}$$

with $\Psi_{11},\Psi_{11}^{-1},\Psi_{21},\Psi_{22},\Psi_{22}^{-1}$ stable. Then the transformed non-linear operator and LTI-system

$$\widetilde{\Delta}=\Psi_{21}\Psi_{11}^{-1}+\Psi_{22}\circ\Delta\circ\Psi_{11}^{-1},\qquad \widetilde{G}=\Psi_{11}G(\Psi_{22}+\Psi_{21}G)^{-1}, \tag{26}$$

give an equivalent loop $(G,\Delta)\cong(\widetilde{G},\widetilde{\Delta})$, where the IQC is transformed to a Small-Gain condition $|\widetilde{\Delta}(\widetilde{v})|_2\le|\widetilde{v}|_2$, $\|\widetilde{G}\|_\infty<1$, now with $\widetilde{\Delta}$ and $\widetilde{G}$ of the same dimension as Δ,G. Since $\|G_e\|_\infty<1$ is equivalent to $\|\widetilde{G}\|_\infty<1$ in the case (25), Theorem 2 implies:

Corollary 2. (Triangular transform). *Suppose a non-linearity Δ can be loop transformed to a L_2-contraction $\widetilde{\Delta}$ in (26) using a lower triangular factorization (25). Suppose the transformed* LTI*-system $\widetilde{G}=\Psi_{11}G\left(I+\Psi_{22}^{-1}\Psi_{21}G\right)^{-1}\Psi_{22}^{-1}$ is stable and satisfies $\|\widetilde{G}\|_\infty<1$. Then the loop (G,Δ) is stable in the L_2-sense.* □

This may also be seen from (16); see also Fig. 9. For upper triangular Ψ we obtain the analogous result with

$$\widetilde{\Delta}=\Psi_{22}\Delta\circ(\Psi_{12}\Delta+\Psi_{11})^{-1},\quad \widetilde{G}=(\Psi_{11}G+\Psi_{12})\Psi_{22}^{-1}. \tag{27}$$

These results no longer require any reference to IQCs or multipliers.

4.2. **Extending the mixed peak-gain/H_∞-program.** The one-dimensional peak-gain norm [20] allows several extensions to MIMO systems, because we can replace the absolute value $|x|$, $x \in \mathbb{R}$, by any of the equivalent vector norms in $\mathbb{R}^n$. If we define a signal norm on $L_\infty([0,\infty),\mathbb{R}^n)$ by

$$|x|_{\infty,p} = \sup_{t\geq 0} |x(t)|_p$$

with $|v|_p$ the p-norm of $v \in \mathbb{R}^n$, $1 \leq p \leq \infty$, then with the notation adopted from [24] *any* induced system norm

$$\|G\|_{(\infty,p),(\infty,q)} = \sup_{x\neq 0} \frac{|G*x|_{\infty,q}}{|x|_{\infty,p}} \tag{28}$$

is a valid MIMO extension of $\|\cdot\|_{\text{pk\_gn}}$. The peak-gain norm, to which we give preference here, is the special case $\|G\|_{\text{pk\_gn}} = \|G\|_{(\infty,\infty),(\infty,\infty)}$, but all norms (28) are equivalent.

Theorem 3. *Suppose the non-linear operator in* (14) *satisfies* $|\Delta(t,x)|_p \leq |x|_q$ *for every* $|x|_q > M$ *and* $|\Delta(t,x)|_p \leq L$ *for every* $|x|_q \leq M$. *If the LTI-system* G *satisfies* $\|G\|_{(\infty,p),(\infty,q)} < 1$, *then the closed loop is BIBO-stable with* $|v|_{\infty,q} + |w|_{\infty,p} \leq k_1(|e|_{\infty,p} + |f|_{\infty,q}) + k_2$ *for all* $e, f \in L_{\infty e}$.

Proof: Put $\Delta_1(t,x) = \Delta(t,x)\chi_{\{|x|_q\leq M\}}(x)$, $\Delta_2(t,x) = \Delta(t,x)\chi_{\{|x|_q>M\}}(x)$, then we have $\sup_{t\geq 0}|\Delta_1(t,v(t))|_p \leq L$, while $\sup_{t\geq 0}|\Delta_2(t,v(t))|_p \leq \sup_{t\geq 0}|v(t)|_q$ by hypothesis. Hence, assuming $|Gx|_{\infty,q} \leq (1-\delta)|x|_{\infty,p}$ for some $0 < \delta < 1$,

$$\begin{aligned}
|v|_{\infty,q} &\leq |w'|_{\infty,q} + |f|_{\infty,q} \\
&\leq |G\Delta_1(v)|_{\infty,q} + |G\Delta_2(v)|_{\infty,q} + |Ge|_{\infty,q} + |f|_{\infty,q} \\
&\leq \|G\|_{(\infty,p)(\infty,q)}\,(|\Delta_1(v)|_{\infty,p} + |\Delta_2(v)|_{\infty,p} + |e|_{\infty,p}) + |f|_{\infty,q} \\
&\leq (1-\delta)L + (1-\delta)|v|_{\infty,p} + (1-\delta)|e|_{\infty,p} + |f|_{\infty,q}
\end{aligned}$$

hence

$$\delta|v|_{\infty,q} \leq (1-\delta)|e|_{\infty,p} + |f|_{\infty,q} + (1-\delta)L.$$

On the other hand

$$|w|_{\infty,p} \leq |\Delta_1(v)|_{\infty,p} + |\Delta_2(v)|_{\infty,p} + |e|_{\infty,p} \leq L + |v|_{\infty,q} + |e|_{\infty,p}.$$

Combining the two implies the estimate. □

For this result compare the more general [42], [66]. The above proof is standard and included for convenience. This gives us now a clue how to extend asymptotic constraints as encountered in Section 2.1 to MIMO non-linearities.

Definition 4. (Asymptotic L_∞-contraction). A non-linear operator $\Delta : [0,\infty) \times \mathbb{R}^n \to \mathbb{R}^n$ is called an asymptotic L_∞-contraction if there exist $L, M > 0$ such that $|\Delta(t,x)|_\infty \leq |x|_\infty$ for all $|x|_\infty > M$, $t \geq 0$, and $|\Delta(t,x)|_\infty \leq L$ for all $|x|_\infty \leq M, t \geq 0$.

Remark 8. The proof of Theorem 3 shows that an asymptotic L_∞-contraction satisfies $|\Delta(t,x)|_\infty \leq |x|_\infty + k$ for all x. Conversely, suppose we have $|\Delta(t,x)|_\infty \leq |x|_\infty + k$ for all x. Then for every $\epsilon > 0$ there exists $M > 0$ such that $|\Delta(t,x)|_\infty < (1+\epsilon)|x|_\infty$ for all $|x|_\infty > M$. For suppose on the contrary that there exist x_n with $|x_n|_\infty \to \infty$ such that for some $\epsilon > 0$ $|\Delta(t,x_n)|_\infty \geq (1+\epsilon)|x_n|_\infty$, then $1+\epsilon \leq |\Delta(t,x_n)|_\infty/|x_n|_\infty \leq 1 + k/|x_n|_\infty \to 1$, a contradiction. Since for the LTI-system we request the strict inequality $\|G\|_{\text{pk\_gn}} < 1$, both conditions for Δ may be used indifferently in the small gain theorem.

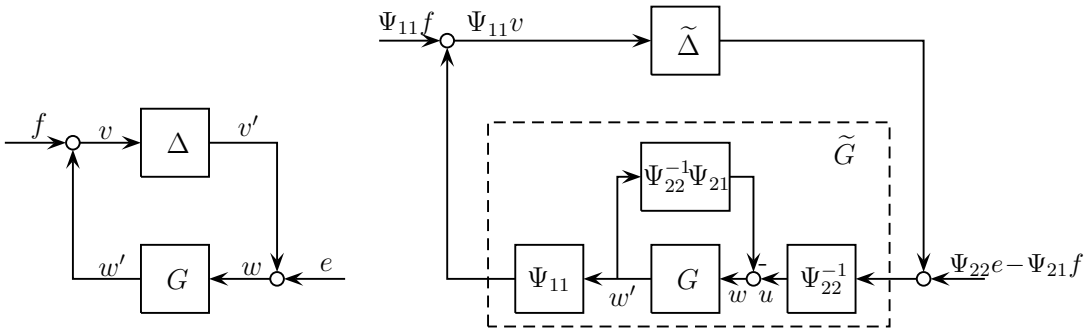

FIGURE 9. Loop-transformation (G, Δ) to $(\widetilde{G}, \widetilde{\Delta})$.

Corollary 3. (Triangular transform). *Let (G, Δ) be L_∞ well-posed, and suppose Δ can be loop-transformed via a lower triangular L_∞-bistable Ψ to an asymptotic L_∞-contraction $\widetilde{\Delta}$. Suppose $\widetilde{G} = \Psi_{11}G(\Psi_{22} + \Psi_{21}G)^{-1}$ is L_∞ well-posed and satisfies $\|\widetilde{G}\|_{\mathrm{pk\_gn}} < 1$. Then the loop* (14) *is BIBO-stable.*

Proof: This refers to (26) shown in Fig. 9, where (G, Δ) is loop transformed to $(\widetilde{G}, \widetilde{\Delta})$ in such a way that BIBO-stability of (G, Δ) is equivalent to BIBO-stability of $(\widetilde{G}, \widetilde{\Delta})$. But $(\widetilde{G}, \widetilde{\Delta})$ is amenable to Theorem 3, hence $\|\widetilde{G}\|_{\mathrm{pk\_gn}} < 1$ implies BIBO-stability of the loop. □

We now extend program (8) to the MIMO-case. In the case of Fig. 2, we transform the non-linearity Δ to an asymptotic contraction $\widetilde{\Delta}$ via (26). Now consider a plant

$$P : \begin{bmatrix} q \\ z \\ y \end{bmatrix} = \begin{bmatrix} P_{11} & 0 & P_{13} \\ 0 & P_{22} & P_{23} \\ P_{31} & P_{32} & P_{33} \end{bmatrix} \begin{bmatrix} p \\ w \\ u \end{bmatrix}, P_1 = \begin{bmatrix} P_{11} & P_{13} \\ P_{31} & P_{33} \end{bmatrix}, P_2 = \begin{bmatrix} P_{22} & P_{23} \\ P_{32} & P_{33} \end{bmatrix}$$

then the extension of (8) has the form of the mixed program

$$(8'') \qquad \begin{array}{ll} \text{minimize} & \|\mathcal{F}_l(P_1, K)^\sim\|_{\mathrm{pk\_gn}} \\ \text{subject to} & \|\mathcal{F}_l(P_2, K)\|_\infty \leq (1+\tau)\gamma_\infty \\ & K \in \mathscr{K} \end{array}$$

where $\sim$ indicates that the loop transformation $\widetilde{G}$ of Fig. 9 is applied to the controlled system $\mathcal{F}_l(P_1, K)$. The program is successful as soon as a structured LTI controller $K^* \in \mathscr{K}$ is found which stabilizes P_1 in the BIBO-sense, stabilizes P_2 exponentially, and achieves $\|\mathcal{F}_l(P_1, K^*)^\sim\|_{\mathrm{pk\_gn}} < 1$.

Remark 9. We could also use the general loop transformation (23). Suppose Δ is obtained from a $|\cdot|_\infty$ contraction Δ_e via (23), where $\Delta_e \star \mathcal{B}$ is L_∞-well-posed. Then a sufficient condition for BIBO-stability of the loop is L_∞-well-posedness of G_e in (20) with $\|G_e\|_{\mathrm{pk\_gn}} < 1$, and this includes both cases (26), (27).

4.3. **Asymptotic L_∞-contractions.** In this section, we collect a variety of examples of MIMO non-linearities which may be assessed by way of asymptotic L_∞-contractions.

Example 1. Consider a non-linearity $\Delta(t, q)$ in loop (G, Δ) as

$$G : \begin{array}{l} \dot{x} = Ax + Bp \\ q = Cx \end{array} \qquad p(t) = \Delta(t, q(t)).$$

We say that Δ is asymptotically polyhedral, if there exist polyhedral norms $|\cdot|_\square$ and $|\cdot|_\triangle$ on $\mathbb{R}^n$ and $k>0$ such that $|\Delta(t,q)|_\square \le |q|_\triangle + k$ for all $q\in\mathbb{R}^n$ and all $t\ge 0$. Now polyhedral norms are of the form

$$|x|_\square = \sup_{i=1,\dots,m}\left|\sum_{j=1}^n \tau_{ij}x_j\right| = |Tx|_\infty, \qquad |y|_\triangle = \sup_{k=1,\dots,p}\left|\sum_{j=1}^n \sigma_{kj}y_j\right| = |Sy|_\infty$$

for certain $T\in\mathbb{R}^{m\times n}$, $S\in\mathbb{R}^{p\times n}$ with $\{x\in\mathbb{R}^n : |Tx|_\infty\le 1\}, \{y\in\mathbb{R}^n : |Sy|_\infty\le 1\}$ bounded. The latter means T,S are injective. Let T^+, S^+ be left inverses, $T^+Tp=p$, $S^+Sq=q$. Then we have

$$|T\Delta(t,S^+Sq)|_\infty = |T\Delta(t,q)|_\infty \le |Sq|_\infty + k$$

so on introducing the new variables $q_1=Sq$, $p_1=Tp$, we have a new non-linearity $\widetilde{\Delta}(t,\cdot) = T\circ\Delta(t,\cdot)\circ S^+$ which satisfies $|\widetilde{\Delta}(t,q_1)|_\infty \le |q_1|_\infty + k$ for all q_1 and $t\ge 0$.

The non-linearity Δ being in loop with G, we transform this to bring $\widetilde{\Delta}$ in loop with:

$$\widetilde{G}: \quad \begin{aligned} \dot{x} &= Ax + BT^+p_1 \\ q_1 &= SCx \end{aligned}$$

This means the non-linear loop (G,Δ) is BIBO-stable if $\|\widetilde{G}\|_{\mathrm{pk\_gn}}<1$. This is a special case of the transform (26).

Example 2. The following is a concretization. We call Δ differentiable at infinity if there exists a matrix $\Delta_\infty := \Delta'(\infty)\in\mathbb{R}^{n\times n}$ such that

$$\lim_{|x|\to\infty}\frac{|\Delta(t,x)-\Delta'(\infty)x|}{|x|}=0$$

uniformly over $t\ge 0$. Here we may choose arbitrary norms in numerator and denominator. Consider the case where $\Delta'(\infty)\neq 0$ and choose regular matrices $T,S\in\mathbb{R}^{n\times n}$ such that $T\Delta'(\infty)S^{-1} = \mathrm{diag}(1-\epsilon,\dots,1-\epsilon,0,\dots,0) =: J_\epsilon$, where the diagonal has $\mathrm{rank}(\Delta'(\infty))$ many entries $1-\epsilon$. Now choose the norms $|y|_\square = |Ty|_\infty$ and $|x|_\triangle = |Sx|_\infty$, then

$$\begin{aligned} \frac{|\Delta(t,x)|_\square}{|x|_\triangle} &\le \frac{|\Delta(t,x)-\Delta'(\infty)x|_\square}{|x|_\triangle} + \frac{|\Delta'(\infty)x|_\square}{|x|_\triangle} \\ &= o(1) + \frac{|T\Delta'(\infty)S^{-1}Sx|_\infty}{|Sx|_\infty} \\ &\le o(1) + \frac{\|J_\epsilon\|_\infty |Sx|_\infty}{|Sx|_\infty} \le o(1) + 1 - \epsilon, \end{aligned}$$

where $\|J_\epsilon\|_\infty = 1-\epsilon$ is the maximum row sum norm. Choosing $M>0$ such that $|o(1)|<\epsilon/2$ for $|x|_\triangle > M$, we arrive at $|\Delta(t,x)|_\square \le (1-\epsilon/2)|x|_\triangle + \sup\{|\Delta(t,x)|_\square : |x|_\triangle\le M\} =: (1-\epsilon/2)|x|_\triangle + k$. This means every non-linearity which is differentiable at infinity admits asymptotic L_∞-constraints.

Remark 10. Suppose a non-linearity $\Delta:[0,\infty)\times\mathbb{R}^n\to\mathbb{R}^n$ satisfies $|\Delta(t,q)|_2\le |q|_2+k$ for some $k\ge 0$ and all $q\in\mathbb{R}^n$, $t\ge 0$. Then in Theorem 3 we would prefer the system norm $\|G\|_{(\infty,2),(\infty,2)}$. Unfortunately, no computable expression is currently known for this norm, so its optimization is presently impossible.

Remark 11. For the case $|\Delta(t,q)|_2\le |q|_2+k$ we have the following makeshift alternative. Choose approximations $P_1\subset B(0,1)\subset P_2$ by polytopes P_1,P_2, then $\Delta(P_1)\subset P_2$ asymptotically, so we are in the situation of Example 1 and we may work with $\|\cdot\|_{\mathrm{pk\_gn}}$. In the case $|\Delta(t,q)|_2\le(1-\epsilon)|q|_2+k$ we may even obtain this with $P_1=P_2\subset\{q:|q|_2=1\}$.

Example 3. MIMO sectors are defined via symmetric matrices $A, B \in \mathbb{S}^n$ satisfying $A \prec B$. A mapping $\phi : \mathbb{R}^n \to \mathbb{R}^n$ with $\phi(0) = 0$ is in the sector $\mathbf{sect}(A, B)$, noted $\phi \in \mathbf{sect}(A, B)$, if $(\phi(x) - Ax)^T(\phi(x) - Bx) \leq 0$ for all $x \in \mathbb{R}^n$.

With the choice $R = \frac{1}{2}(B - A) \succ 0$ and $C = \frac{1}{2}(B + A)$ we find that $\psi(x) = \phi(x) - Cx$ satisfies $\psi(x)^T\psi(x) \leq x^T R^T Rx$, so we get a norm bound $|\psi(x)|_2 \leq |Rx|_2$, and if we define $\Delta = \psi \circ R^{-1} = (\phi - C) \circ R^{-1}$, then $|\Delta(y)|_2 \leq |y|_2$. When we allow $|\Delta(y)|_2 \leq |y|_2 + k$ for some $k \geq 0$ and all y, this is a typical application of the two previous remarks, where we would like to apply Theorem 3 with $\|\cdot\|_{(\infty,2),(\infty,2)}$.

Example 4. As a concretization [64, 18] consider a non-linearity ϕ generated by a convex quadratic program:

$$\phi(x) = \operatorname{argmin}\{\tfrac{1}{2}v^T Hv - v^T x : Lv \leq b\} \tag{29}$$

where $H \succ 0$ and $L \in \mathbb{R}^{m\times n}$, $b \geq 0, b \in \mathbb{R}^m$ are fixed, and optimization is over $v \in \mathbb{R}^n$. Using the Kuhn-Tucker conditions one verifies that ϕ satisfies the MIMO sector bound

$$\phi(x)^T(H\phi(x) - x) \leq 0 \text{ for all } x.$$

Then from the above $\psi(x) = 2H^{1/2}\phi(H^{1/2}x) - x$ is a $|\cdot|_2$-contraction. This means an asymptotic quadratic constraint for ϕ would lead to $\|\cdot\|_{(\infty,2),(\infty,2)}$, which is, however, not available for computations. A polyhedral approximation based on Remark 11 may be used instead.

Example 5. (Continued). In the above case we can bring in $\|G\|_{\text{pk\_gn}}$ directly, because the solution mapping of a convex quadratic program with perturbation of the linear term or the constraints is known to be piecewise affine [17, 18], so it maps polyhedra to polyhedra. This allows a construction as in Example 1.

Since $H \succ 0$, (29) is equivalent to projecting $H^{-1}x$ orthogonally on the polyhedron $\{v : Lv \leq b\}$ with regard to the Euclidean norm $|x|_H^2 = x^T Hx$. Let $I \subset \{1, \dots, m\}$, $J = \{1, \dots, m\} \setminus I$, so that $F = \{v \in \mathbb{R}^n : L_I v = b_I, L_J v \leq b_J\}$ is a face of the polyhedron, then projection of x on F is obtained as

$$\phi(x) = H^{-1}\left(x - L_I^T(L_I H^{-1} L_I^T)^{-1}\left[L_I H^{-1}x - b_I\right]\right)$$

using generalized least squares. This shows that ϕ is piecewise affine.

Example 6. (Piecewise affine). A non-linearity ϕ on $\mathbb{R}^n$ is *piecewise affine* if there exist finitely many non-overlapping polyhedra $P_1, \dots, P_N$ with $\bigcup_{i=1}^N P_i = \mathbb{R}^n$ such that $\phi|P_i$ is affine, i.e. there exist an affine mapping $A_i(x) = b_i + L_i x$ with $A_i|P_i = \phi|P_i$. Here L_i is the linear part of A_i. For each polyhedron P_i choose a Motzkin decomposition $P_i = Q_i + C_i$ with Q_i a polytope and C_i a polyhedral cone. Let $B_\triangle = \{x : |x|_\triangle \leq 1\}$ be the unit ball of a polyhedral norm, compute the polytopes $B_i = B_\triangle \cap C_i$ and $B_i' = L_i(B_i)$. (Note that $L_i(C_i)$ is a polyhedral cone, so if it is bounded, it reduces to $\{0\}$, in which case $B_i' = \{0\}$, too. Therefore only unbounded $L_i(C_i)$ have to be considered). Finally let B' be the convex hull of $\bigcup_{i=1}^N B_i'$, then B' is a polytope containing 0. Let $k_1 = \max\{|b'|_\infty : b' \in B'\}$.

We claim that there exists a constant $k > 0$ such that for every $x \in \mathbb{R}^n$, $\phi(x) \in |x|_\triangle B' + kB_\infty$. Indeed, let $x \in P_i$, $x = y + z$ with $y \in Q_i$, $z \in C_i$. Then $\phi(x) = b_i + L_i x = b_i + L_i y + L_i z = b_i + L_i y + |z|_\triangle L_i(z/|z|_\triangle) = b_i + L_i y_i + |z|_\triangle b'$ for some $b' \in B_i'$, using the fact that $z/|z|_\triangle \in B_\triangle \cap C_i$, hence $L_i(z/|z|_\triangle) \in L_i(B_\triangle \cap C_i) = B_i'$.

Now $|z|_\triangle = |x - y|_\triangle \leq |x|_\triangle + |y|_\triangle$, hence $|z|_\triangle b' = (|x|_\triangle + |y|_\triangle)\rho b'$ for some $\rho \in [0, 1]$, and since $0 \in B_i'$, we have $\rho b' = b'' \in B_i'$. Then $|z|_\triangle b' = |y|_\triangle b'' + |x|_\triangle b''$.

Altogether $\phi(x) = b_i + L_i y + |y|_\triangle b'' + |x|_\triangle b''$, and here the term $b_i + L_i y + |y|_\triangle b''$ is bounded independently of $|x|_\triangle$, because $y \in Q_i$ are bounded. We put $k_2 = \max_{i=1,\dots,N} |b_i|_\infty$, $k_3 = \max_{i=1,\dots,N} \max_{y\in Q_i} |L_i y|_\infty$ and $k_4 = \max_{i=1,\dots,N} \max_{y\in Q_i} |y|_\infty$, then $k = k_2 + k_3 + k_1 k_4$.

Now let $B_\square = \mathrm{co}(B' \cup (-B'))$, then $B_\square$ is a symmetric polytope, hence its Minkowski functional is a polyhedral norm, $|\cdot|_\square$, and we have shown $|\phi(x)|_\square \le |x|_\triangle + k$ for all x. The matrix T defining $|\cdot|_\square$ can be obtained from the polyhedral representation $B' = \{x : Tx \le 1\}$, which for moderate dimensions of x can be pre-computed. The matrix S is obtained from $|x|_\triangle = |Sx|_\infty$.

Example 7. We consider a numerical example with a non-linearity based on (29). The parametric quadratic program

$$(P)_q \quad \begin{array}{ll} \text{minimize} & \frac{1}{2}x_1^2 + \frac{1}{2}x_2^2 - q_1x_1 - q_2x_2 \\ \text{subject to} & x_1 - x_2 \le 3 \\ & x_1 + x_2 \ge 0 \\ & x_1 \ge 0 \\ & x_2 \ge -1 \end{array}$$

defines a non-linear operator $\phi : \mathbb{R}^2 \to \mathbb{R}^2$ via $p = \mathrm{argmin}(P)_q$. Here $p = \phi(q)$ is the orthogonal projection of q on the polyhedron $P = \{x \in \mathbb{R}^2 : Lx \le b\}$, where $L^T = \begin{bmatrix} 1 & -1 & -1 & 0 \\ -1 & -1 & 0 & -1 \end{bmatrix}$, $b^T = \begin{bmatrix} 3 & 0 & 0 & 1 \end{bmatrix}$. For every face F of P the set $F' = \phi^{-1}(F)$ is a polyhedron and each $\phi|F' : F' \to P$ is affine. Here P has 8 faces, three vertices, four facets, and P itself. The unbounded faces are $F_1 = \{(2,-1)\} + \mathbb{R}_+(1,1) = Q_1 + C_1$, $F_2 = \mathbb{R}_+(0,1) = C_2$, and $P = Q + 0^+P$, with $0^+P = \{x : Lx \le 0\}$. Now $F_1' = \phi^{-1}(F_1) = \{(2,-1)\} + \mathbb{R}_+(1,1) + \mathbb{R}_+(1,-1) = Q_1 + C_1'$ and $\phi_1 = \phi|F_1' = A_1|F_1'$ for the affine mapping $A_1(x) = L_1x + b_1 = \begin{bmatrix} 1/2 & 1/2 \\ 1/2 & 1/2 \end{bmatrix}\begin{bmatrix} x_1 \\ x_2 \end{bmatrix} + \begin{bmatrix} 3/2 \\ -3/2 \end{bmatrix}$. Similarly, $F_2' = \phi^{-1}(F_2) = \mathbb{R}_+(-1,0) + \mathbb{R}_+(0,1) = C_2'$, and $\phi_2 = \phi|F_2' = A_2|F_2'$ for the affine mapping $L_2x = A_2(x) = \begin{bmatrix} 0 & x_2 \end{bmatrix}^T$, which is already linear. Clearly, $\phi^{-1}(P) = P$ and $\phi_3 = \phi|P = I|P = L_3$. Now consider the box $B_\infty = \{x \in \mathbb{R}^2 : |x_1| \le 1, |x_2| \le 1\}$, then $L_1(B_\infty \cap F_1') = [(0,0),(1,1)]$ is a segment. Similarly $L_2(B_\infty \cap F_2') = [(0,0),(0,1)]$. Moreover, $L_3(B_\infty \cap 0^+P) = B_\infty \cap 0^+P$. The convex hull of the union of these three polytopes is $B' = \mathrm{co}\{(0,0),(0,1),(1,1)\}$. Hence we have $B = \mathrm{co}(B' \cup (-B')) = \mathrm{co}\{(-1,-1),(0,1),(1,1),(0,-1)\}$. The construction shows $|\phi(q)|_\square \le |q|_\infty + k$ for every q, where $|x|_\square = |Tx|_\infty$ is the polyhedral norm generated by B, obtained with $T = \begin{bmatrix} 2 & -1 \\ 0 & 1 \end{bmatrix}$.

Now observe that instead of the $|\cdot|_\infty$-unit ball B_∞ we can choose a larger polytope $B_\triangle$, which still satisfies $L_i(B_\triangle \cap F_i') \subset B'$. Namely, we can take $B_\triangle = \mathrm{co}(B_\infty \cup \{(2,0),(-2,0)\})$. The polyhedral norm is $|q|_\triangle = |Sq|_\infty$ with $S^T = \begin{bmatrix} 0 & 1/2 & 1/2 \\ 1 & 1/2 & -1/2 \end{bmatrix}$. By example 1, BIBO-stability of

$$G : \quad \begin{array}{l} \dot{x} = Ax + Bp \\ q = Cx \end{array} \qquad\qquad p(t) = \phi(q(t)).$$

can now be assessed via BIBO-stability of

$$\widetilde{G} : \quad \begin{array}{l} \dot{x} = Ax + BT^{-1}p_1 \\ q_1 = SCx \end{array} \qquad\qquad p_1(t) = T\phi(S^+q_1(t)),$$

where $T \circ \phi \circ S^+$ is a $|\cdot|_\infty$-contraction. A sufficient condition for BIBO-stability of the loop is therefore $\|\widetilde{G}\|_{\mathrm{pk\_gn}} < 1$.

We compare this to the sector characterization of the non-linearity ϕ from example 3. With $H = I_2$ we get $\phi(q)^T(\phi(q) - q) \le 0$, hence $\psi(q) = 2\phi(q) - q$ is an L_2-contraction.

This leads to

$$\widehat{G}: \quad \begin{matrix} \dot{x} = Ax + \frac{1}{2}BCx + \frac{1}{2}B\widehat{p} \\ \widehat{q} = Cx \end{matrix} \qquad\qquad \widehat{p}(t) = \psi(\widehat{q}(t)),$$

whence a sufficient condition for L_2-stability is $\|\widehat{G}\|_{L_\infty} < 1$, and this can also be obtained from the circle criterion. Choosing

$$A = \begin{bmatrix} -1 & 2 \\ 0.001 & -3 \end{bmatrix}, B = \begin{bmatrix} 2 & -1 \\ 0 & 1 \end{bmatrix}, C = \rho \begin{bmatrix} 1 & 0 \\ 1 & 1 \end{bmatrix}$$

we get two curves $n_1(\rho) = \|\widetilde{G}_\rho\|_{\mathrm{pk\_gn}}$ and $n_2(\rho) = \|\widehat{G}_\rho\|_\infty$. We have $n_1(0.499) = 0.9988$, $n_2(0.499) = 1.2597$, $n_1(0.434) = 0.8687$, $n_2(0.434) = 0.9995$, so in between these two values the test $\|\widetilde{G}\|_{\mathrm{pk\_gn}} < 1$ guarantees BIBO-stability, while the circle criterion fails to prove L_2-stability.

Example 8. Multi-dimensional saturation is not always suitably seized by the Euclidean norm [51]. For signals $x(t) \in \mathbb{R}^n$ consider a convex polytope P of dimension n with the origin in its interior, and let $\mu_P(x) = \inf\{\mu \geq 0 : x \in \mu P\}$ be its gauge function. Then a structured saturation operator is $\mathrm{sat}_P(x) = x$ for $\mu_P(x) \leq 1$, $\mathrm{sat}_P(x) = x/\mu_P(x)$ for $\mu_P(x) > 1$. In other words, if $x(t) \in P$, then the signal is unaffected by saturation, but if $x(t)$ reaches the boundary of P, then along every ray ρx, $\rho > 0$, the magnitude of the signal is frozen at the value it had attained when crossing the boundary of P, while the direction of the signal is unchanged. This is now a special case of Example 1.

Example 9. A typical case is signal clipping, where $y = \sigma(x)$ is given as $y_i = \mathrm{sign}(x_i)$ if $|x_i| > 1$, $y_i = x_i$ otherwise. Here $B' = B_\infty$. Indeed, consider for simplicity the case $n = 2$. Then σ is piecewise affine with 9 different polytopes $P_1, \dots, P_9$, where $P_9 = B_\infty$, $P_1 = \{(x_1, x_2) : -1 \leq x_1 \leq 1, x_2 \geq 1\}$, $P_2 = \{(x_1, x_2) : x_1 \geq 1, x_2 \geq 1\}$, $P_3 = \{(x_1, x_2) : x_1 \geq 1, -1 \leq x_2 \leq 1\}$, etc. We have $A_1(x) = (x_1, 1)$, $Q_1 = [-1, 1) \times \{0\}$, $C_1 = \{0\} \times \mathbb{R}_+$, $A_2(x) = (1, 1)$, $Q_2 = \{(1, 1)\}$, $C_2 = \mathbb{R}^+ \times \mathbb{R}^+$, $C_2' = \{(0, 0)\}$, etc. So only the four facets among the 9 faces of B_∞ contribute to B'.

This immediately applies to systems like $\dot{x} = \sigma(Ax + b)$ or $\dot{x} = \sigma(Ax + Bu)$ etc. as for instance considered in [63].

Example 10. The authors of [47] consider non-linear systems $\dot{x} = \sum_{i=1}^N \mu_i(x, u)\,[A_i x + B_i u]$, where $\mu_i(x, u) \geq 0$, $\sum_{i=1}^N \mu_i(x, u) = 1$. This can be modeled by an operator $p = \phi(q) := \sum_{i=1}^N \mu_i(q) q_i$ with $\mu_i(q)$ a convex combination, so that $|\phi(q)|_1 \leq |q|_\infty$, which is a polyhedral non-linearity.

Example 11. (Attractors, limit cycles, chaotics). In [46] the authors generate MIMO non-linearities Δ by putting LTI-systems H in feedback with a static non-linearities Φ. This leads to attractors, limit cycles, chaotic behavior, and much else. Some of these may be considered special cases of (27). The out-set is a dynamic system $z = \Delta(w)$:

$$H: \quad \begin{matrix} \dot{x} = Ax + Bp + Bw \\ q = Cx, \quad z = x, \end{matrix} \qquad p = \Phi(q) \qquad \Delta = (H, \Phi) \tag{30}$$

where $\Phi(0) = 0$. If $|\Phi(q)|_\infty \leq r|q|_\infty + k$ asymptotically, then by Theorem 3, BIBO-stability of Δ follows from $\|H\|_{\mathrm{pk\_gn}} < r^{-1}$. In particular, if Φ has bounded range, then we can choose $r > 0$ arbitrarily, hence $\|H\|_{\mathrm{pk\_gn}} < \infty$ gives BIBO-stability of Δ.

For instance, similar to [46, Example 4.6] we let $\Phi(q_1,q_2,q_3)=(\phi(q_3),0,0)$ with $\phi(q)=a\tanh(kq)+\rho q$, $B=C=I_3$, and

$$A=\begin{bmatrix}-(\beta_1+\beta_2+\beta_3) & -(\beta_1\beta_2+\beta_1\beta_3+\beta_2\beta_3)/M & -\beta_1\beta_2\beta_3/M\\ M & 0 & 0\\ 0 & 1 & 0\end{bmatrix}.$$

For $M=a=k=10$, $\rho=0.3$, $\beta_1=2$, $\beta_2=3$, $\beta_3=5$, the non-linearity Δ has three steady states, the unstable 0, and two stable attractors $(0,0,\pm 2.963)$ (Fig. 10 left). The system is globally BIBO-stable, because ϕ has slope ρ at infinity, so integrating ρq_3 into the system H gives H_0 in loop with a non-linearity Φ_0 of bounded range. Then $r=1/3$ gives $\|H_0\|_{\text{pk\_gn}}=2.0759<3=r^{-1}$. The linearization of Δ at 0 has system matrix $A+E_1$ with $E_1=\big[0,0,\phi'(0);0,0,0;0,0,0\big]$, which is unstable, but a stable linearization can readily be obtained by linearizing about one of the attractors, e.g. $\bar x=(0,0,2.963)$.

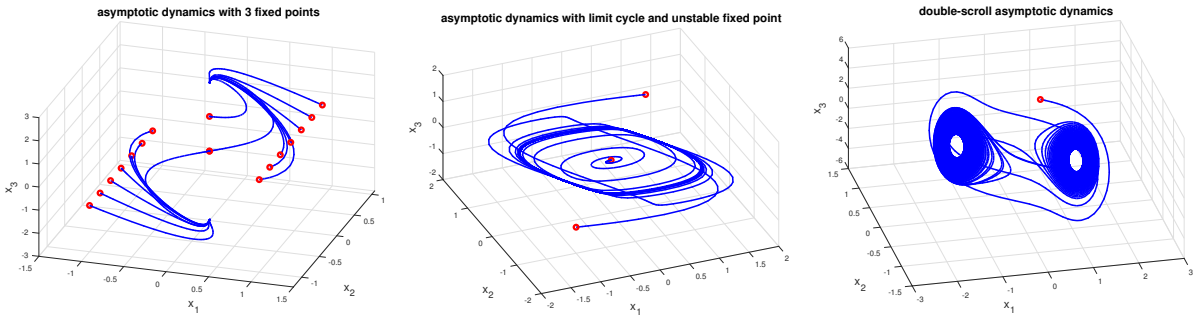

FIGURE 10. Two attractors and unstable origin (left), limit cycle (middle), chaotic double scroll (right).

A different case has $a=-10$, where the origin is an unstable steady state and an attracting limit cycle occurs (Fig. 10 middle). Global BIBO-stability of the loop follows again from $\|H\|_{\text{pk\_gn}}<\infty$, but a stable linearization now requires a modified LTI-system, where the limit cycle is subtracted from H to get a stable steady state.

In those cases, where $z=\Delta(w)$ is BIBO-stable, we can consider it in loop with a tunable LTI-system G as in Fig. 9. For unstable H we can still apply the results of section 4.2 when H is stabilized by feedback with a tunable G, now considering Φ in loop with $\mathcal{F}_l(H,G)$:

Proposition 2. *Let $z=\Delta(w)$ in (30) be in upper feedback with an LTI-system G as in (14). Suppose Φ satisfies an asymptotic constraint $|\Phi(q)|_\infty\le r|q|_\infty+k$. Then a sufficient condition for global BIBO-stability of the loop (G,Δ) is $\|\mathcal{F}_l(H,G)\|_{\text{pk\_gn}}<r^{-1}$.*

Example 12. (Attractors ... continued). An interesting study in this line is Chua's circuit [43], see [46, 5.4], where

$$A=\begin{bmatrix}-\alpha & \alpha & 0\\ 1 & -1 & 1\\ 0 & -\beta & 0\end{bmatrix},\ B=C=I_3,\quad \begin{array}{l}\Phi(q)=(\phi(q_1),0,0)\\ \phi(q_1)=\alpha\tanh(2q_1)+\alpha\rho q_1\end{array}$$

For $\alpha=8.3$, $\beta=16.5$, $\rho=0.25$ the double scroll attractor appears (Fig. 10 right). The non-linearity has slope $\alpha\rho$ at infinity. Therefore global BIBO-stability of $\Delta=(H,\Phi)$ follow from stability of $A+E_2$, $E_2=\big[\alpha\rho,0,0;0,0,0;0,0,0\big]$.

A common feature of these examples is that the sector non-linearity invites attempting L_2-stability, which however fails due to the persistence of more than one attractor in feedback. This is where global L_∞-stability is still in business.

Example 13. (Attractors ... continued). We study this phenomenon in more detail through a feedback design example. Consider the MIMO Lur'e system

$$H: \begin{array}{l} \dot{x} = Ax + Bp + B_u u \\ q = Cx, \quad y = C_y x, \end{array} \qquad p = \Phi(q) \tag{31}$$

with $\Phi : \mathbb{R}^3 \to \mathbb{R}^3$ the MIMO static non-linearity

$$\Phi(q) := \begin{bmatrix} \frac{q_1^2}{a_1+q_1^2}(\tanh(c_1 q_1) + \rho_1 q_1)) \\ \frac{q_2^2}{a_2+q_2^2}(\tanh(c_1 q_2) + \rho_2 q_1)) \\ \frac{q_3^2}{a_3+q_3^2}(\tanh(c_3 q_3) + \rho_3 q_3)) \end{bmatrix},$$

with $a_1 = 0.1$, $a_2 = 0.2$, $a_3 = 0.3$, $\rho_1 = 0.1$, $\rho_2 = 0.2$, $\rho_3 = 0.3$, $c_1 = 2$, $c_2 = 3$ and $c_3 = 4$. State-space data are given as

$$A := \begin{bmatrix} -2 & 8.8 & 0 \\ 1 & -1 & 1 \\ 0 & -15 & 0 \end{bmatrix}, B := \begin{bmatrix} 5 & 0 & 0 \\ 0 & 0.1 & 0 \\ 0 & 0 & 0.3 \end{bmatrix}, C := I_3,$$

$$B_u := \begin{bmatrix} 1 \\ 1 \\ 1 \end{bmatrix} \quad C_y := \begin{bmatrix} 1 & 1 & 1 \end{bmatrix}.$$

The uncontrolled linear dynamics show 2 unstable oscillating modes $0.1422 \pm 3.0189i$. Simulations of the uncontrolled non-linear system are shown in Fig. 11 (upper line) with a double-scroll regime close to the origin, and an escaping unstable spiral regime away from 0. Here we regard $\Delta = (H, \Phi)$ as mapping initial conditions $x(0)$ to state x.

Now we investigate whether the system may be stabilized by feedback $u = Ky$ in the L_∞-sense, using the techniques in sections 4.1 and 4.2. As can be seen each component Φ_i belongs to the asymptotic sector $\mathbf{sect}(0, \rho_i + \epsilon)$ for any $\epsilon > 0$. Using section 4.2, we infer that the closed-loop system is L_∞-stable whenever $\|\mathcal{F}_l(\widetilde{H}, K)\|_{\mathrm{pk\_gn}} < r^{-1}$, where and $r := \max\{\rho_1/2, \rho_2/2, \rho_3/2\}$ and $\widetilde{H}$ is obtained from H by centering the non-linearity. The latter amounts to shifting the A-matrix to $A + B\Gamma C$ with $\Gamma := \mathrm{diag}\,(\rho_1/2, \rho_2/2, \rho_3/2)$.

Running program (8) over the class $\mathscr{K}$ of PID controllers leads to

$$K^*(s) := -0.796 + \frac{0.000352}{s} + \frac{0.097}{940s + 1},$$

with the result $\|\mathcal{F}_l(\widetilde{H}, K^*)\|_{\mathrm{pk\_gn}} = 5.34 < r^{-1} = 6.67$, affirming BIBO stability. Closed-loop simulations in Fig. 11 bottom show co-existence of 3 stable equilibrium points at the origin (right) and away from the origin (bottom left) with state-space coordinates $(\pm 2.98, \mp 0.0420, \mp 2.94, \mp 237.94, 0)$.

Note that in this study step 4 of the algorithm fails, because $\Phi_i \in \mathbf{sect}(0, 1.17)$ tightly for every i. Therefore, to get a global L_2-stability certificate it would have been required to determine a PID controller for which the H_∞ norm of the corresponding centered system was less than $1/r_0 = 1.71$, and this value was not achievable in program (7).

5. Peak-to-peak norm

5.1. **Estimate.** It is well-known [24, 27, 33, 20, 21] that for real-rational systems G the peak-gain or peak-to-peak norm is

$$\|G\|_{\mathrm{pk\_gn}} = \max_{i=1,\ldots,m} \sum_{j=1}^{p} \left(|g_{ij}^0|_1 + |d_{ij}| \right), \tag{32}$$

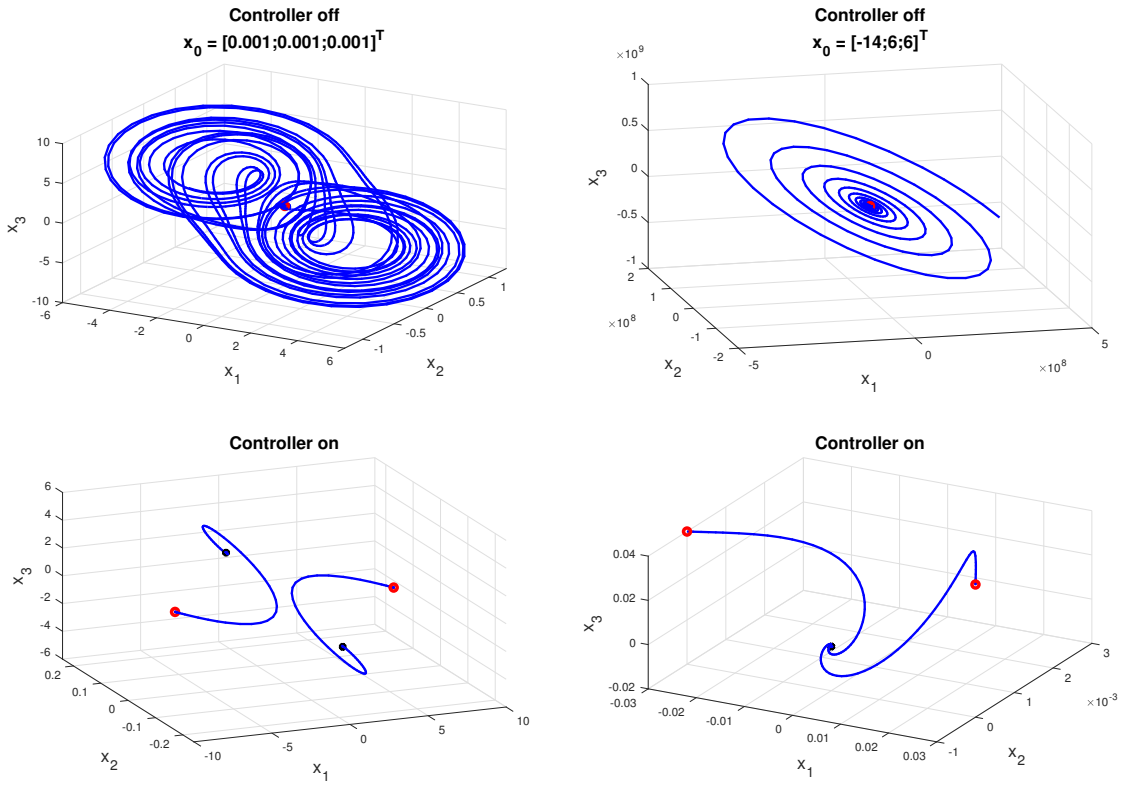

FIGURE 11. Non-linearity $\Delta = (H, \Phi)$ with unstable $H(s)$ shows 2-double scroll (top left) or diverging spiral (top right) for different initial values '•'. Peak-gain optimization with a PID controller gives BIBO-stability of $(K, \Delta) = ((K, H), \Phi)$ with convergence to 3 stable equilibrium points (bottom left and right). '•'.

where $g_{ij}(t) = c_i e^{At} b_j + d_{ij}\delta(t) = g^0_{ij}(t) + d_{ij}\delta(t)$ with $g^0_{ij} \in L_1$. A special case is the well-known expression

$$\|\!|A|\!\|_\infty = \max_{i=1,\dots,m} \sum_{k=1}^{p} |a_{ik}| = \max_{i=1,\dots,m} |\mathrm{row}_i(A)|_1$$

of the maximum row-sum-norm of $A \in \mathbb{R}^{m\times p}$, i.e., the induced ℓ_∞-ℓ_∞ matrix norm.

Formula (32) holds also for infinite dimensional BIBO-stable systems and may be justified e.g. by the approach [67, 37], which considers BIBO-stable systems as all those LTI-systems G, where $G(s)$ is the Laplace transform of a matrix-valued Radon measure of bounded variation. While [67] handles the SISO case, where the norm is referred to as the $\mathcal{M}$-norm $\|\mu\|_{\mathcal{M}} = \sup_{\phi\in\mathscr{D}(\mathbb{R}^+),\|\phi\|_\infty\le 1} \int_{\mathbb{R}^+} \phi d\mu$, one easily generalizes this to the MIMO case and obtains the formula

$$\|G\|_{\mathrm{pk\_gn}} = \sup_{i=1,\dots,m} \sum_{k=1}^{p} \|\mu_{ik}\|_{\mathcal{M}},$$

which contains (32) as a special case. In particular, it was possible to apply it in the slipstick study, because the impulse response was an element of L_1.

Estimate (2) is mentioned in [27] with non-specified constants, and the SISO case $p = m = 1$ is proved in [21, Thm.] for discrete SISO systems, and in [35, pp. 11-12] for continuous SISO systems, where in the latter reference the idea of proof is attributed

to I. Gohberg. The left hand estimate in (2) holds also for infinite dimensional systems, e.g. those where $G(s)$ is the Laplace transform of a Radon measure of bounded variation, while the right hand estimate is true for finite-dimensional G. For strictly proper systems, the estimate $\|G\|_{\mathrm{pk\_gn}} \leq 2np^{1/2}\|G\|_\infty$ is valid. Details on computing these estimates will be published elsewhere.

5.2. **Implementation.** Stand alone computation of the peak-gain norm with high precision has been addressed in the literature [54, 41, 21, 24, 27, 28, 34]. For optimization, due to non-smoothness of both norms in (8), we need to supply subgradients of closed-loop integral functionals $\phi_{ij} : K \to \int_0^\infty |c_i(K)e^{A(K)t}b_j(K)|dt$, those for the H_∞-norm being well-known [7]. Putting $f(K,t) = c(K)e^{A(K)t}b(K)$ and $F(K) = \int_0^\infty |f(K,t)|dt$ for the generic terms, we need partial derivatives $\partial f(K,t)/\partial K_{\mu\nu}$, where $K_{\mu\nu}$ are the controller gains, which depend in turn on the tunable parameters $\mathbf{x}$ over which we ultimately optimize. Since dependence $K_{\mu\nu}(\mathbf{x})$ and $f(K,t)$ are differentiable, non-smoothness occurs only when the absolute value $|f(\cdot,t)|$ is formed, and ultimately via the finite maximum over rows in (32). Subgradients $g(K,t) \in \partial|\cdot| \circ f(K,t)$ are obtained as $g_{\mu\nu}(K,t) = \partial f(K,t)/\partial K_{\mu\nu}\mathrm{sign} f(K,t)$ for $f(K,t) \neq 0$, while those (K,t) where $f(K,t) = 0$ give the full set of subgradients $g_{\mu\nu}(K,t) \in \partial f(K,t)/\partial K_{\mu\nu} \cdot [-1,1]$. Partial derivatives $\partial f/\partial K_{\mu\nu}$ are obtained via algorithmic differentiation [15]. Finally, subgradients $G \in \partial F(K)$ of integral functionals are by regularity simply integrals of pointwise subgradients $G_{\mu\nu}(K) = \int_0^\infty \partial f(K,t)/\partial K_{\mu\nu}\mathrm{sign} f(K,t)dt$ [40, 49, 50].

For mixed programs like (8) it is possible to use a progress function approach as in [60, 61, 62, 30, 31, 32, 38, 14]. Here we rather follow the line [8, 11] suited for norm functionals, where an iteratively re-weighted maximum of several norms is minimized; cf. [3] for an overview, where in particular the concept of hard and soft constraints is addressed. This approach is also used in the `systune` function [39, 2, 72] based on [8], and has been used in our experiments. For convergence issues of bundle and bundle trust-region techniques we refer to [12, 48].

According to the line in [8] program (8) is addressed by minimizing a maximum

$$\min_{\mathbf{x}\in\mathbb{R}^n} \max\left\{\alpha\|T_{wz}(G,K(\mathbf{x}))\|_\infty, \beta\|T_{pq}(G_\psi,K(\mathbf{x}))\|_{\mathrm{pk\_gn}}\right\},$$

where the weights α,β are updated iteratively until the constraint of (8) is satisfied, from where on the objective is reduced. Here $K(\mathbf{x})$ expresses dependence of K on the tunable parameters $\mathbf{x}$. The first term splits into a semi-infinite maximum

$$\|T_{wz}(G,K(\mathbf{x}))\|_\infty = \max_{\omega\in[0,\infty]} \overline{\sigma}(T_{wz}(j\omega,G,K(\mathbf{x}))),$$

whereas the second term, after time-domain discretization, becomes a finite maximum

$$\|T_{pq}(G_\psi,K(\mathbf{x}))\|_{\mathrm{pk\_gn}} = \max_{i=1,\ldots,m} \sum_{j=1}^{p} \left(\sum_{t\in T} \left|c_i(\mathbf{x})e^{A(\mathbf{x})t}b_j(\mathbf{x})\right| + |d_{ij}(\mathbf{x})| \right),$$

with $c_i(\mathbf{x})e^{A(\mathbf{x})t}b_j(\mathbf{x}) + d_{ij}(\mathbf{x})\delta(t)$ the closed loop impulse response of the entry (i,j) of the channel $T_{pq}(G_\psi,K(\mathbf{x}))$. For discretization we have used the method of [54], which is readily extended to the MIMO case.

It is helpful to update the weights α,β in such a way that at the current iterate $\mathbf{x}$ the three branches are at least nearly active. Selecting a set of active and near active frequencies for the first and third criterion is explained in [8, sect. 4.4], and we proceed analogously for the second branch. This strategy to include near-active branches into local models has turned out highly effective, as it avoids stalling at non-optimal points.

6. Conclusion

We have presented a method for stabilization and performance optimization of non-linear controlled systems, where the non-linearity satisfies a sector constraint asymptotically. This leads to global closed-loop BIBO-stability in tandem with local exponential stability in situations where global closed-loop L_2-stability fails, either due to exceedingly large sectors, or more principally, due to persistence of several attracting regimes in closed loop. The new approach requires solving a mixed L_1/H_∞-synthesis program, and uses properties of the L_1- or peak-gain system norm.

References

[1] P. Apkarian. Nonsmooth μ-synthesis. *International Journal of Robust and non-linear Control*, 21(13):2011,1493–1508.

[2] P. Apkarian, P. Gahinet, C. Buhr. Multi-model, multi-objective tuning of fixed-structure controllers. *2014 European Control Conference (ECC)* 2014, 856-861.

[3] P. Apkarian, D. Noll. Optimization-based control design techniques and tools. *Encyclopedia of Systems and Control 2019*. Baillieul, John; Samad, Tariq (Eds.).

[4] P. Apkarian, D. Noll. Boundary feedback control of an anti-stable wave equation. *IMA Journal of Mathematical Control and Information*, 37:2020,1367-1399.

[5] P. Apkarian, D. Noll. Boundary control of partial differential equations using frequency domain optimization techniques. *Systems and Control Letters*, 135:2020,1045-77.

[6] P. Apkarian, D. Noll. Structured H_∞-control of infinite dimensional systems. *Int. J. Robust Nonlin. Control*, 28(9):2018,3212–3238.

[7] P. Apkarian, D. Noll. Nonsmooth H_∞ synthesis. *IEEE Trans. Automat. Control*, 51 (1) (2006) 71–86 (January 2006).

[8] P. Apkarian, D. Noll. Nonsmooth optimization for multidisk H_∞ synthesis. *European J. of Control*, 12 (3):2006,229–244.

[9] P. Apkarian, D. Noll. IQC analysis and synthesis via nonsmooth optimization. *Systems and Control Letters*, 55(12):2006,971 - 981.

[10] P. Apkarian, D. Noll, O. Prot. Nonsmooth methods for control design with integral quadratic constraints. *Proceedings 46th IEEE CDC*, New Orleans 2007.

[11] P. Apkarian, D. Noll, L. Ravanbod. Robustness via structured H_∞/H_∞-synthesis. *International Journal of Control*, 84(5):2011,851-866.

[12] P. Apkarian, D. Noll, L. Ravanbod. Nonsmooth bundle trust-region algorithm with applications to robust stability. *Set-Valued and Variational Analysis*, 24 (1):2016,115–148.

[13] P. Apkarian, D. Noll, L. Ravanbod. Non-smooth optimization for robust control of infinite-dimensional systems. *Set-Valued Var. Anal.*, 26(2):2018,405-429.

[14] P. Apkarian, D. Noll, A. Rondepierre. Mixed H_2/H_∞-control via nonsmooth optimization. *SIAM J. Contr. Optim.*, 47(3):2008,1516-1546.

[15] P. Apkarian, D. Noll, A. M. Simões. Time-domain control design: a non-differentiable approach. *IEEE Transactions on Control Systems Technology*, 17(6):2009,1439 - 1445.

[16] V. Balakrishnan, S. Boyd. On computing the worst case peak gain of linear systems. *Systems and Control Letters*, 19(4):1992,265-269.

[17] B. Bank, J. Guddat, D. Klatte, B. Kummer, K. Tammer. *Non-linear parametric optimization.* Springer Verlag 1983.

[18] A. Bemporad, M. Morari, V. Dua, and E. Pistikopoulos. The explicit linear quadratic regulator for constrained systems. *Automatica*, 38(1):2002,3-20.

[19] B. Besselink, T. Vromen, N. Kremers, N. van de Wouw. Analysis and control of stick-slip oscillations in drilling systems. *IEEE Trans. Control. Syst. Tech.*, 24(5):2016,1582-1593.

[20] S.P. Boyd, C.H. Barratt. *Linear controller design. Limits of performance.* Prentice Hall 1991.

[21] S. Boyd, J. Doyle. Comparison of peak and RMS gains for discrete-time systems. *Systems & Control Letters*, 9:1987,1-6.

[22] V.M.G.B. Cavalcanti, A.M. Simões. IQC-synthesis under structural constraints. *Int. J. Robust Nonlin. Control*, 30:2020,4880-4905.

[23] N. Challamel. Rock destruction effect on the stability of a drilling structure. *Journal of Sound and Vibration*, 233:2000,235-254.

[24] V.S. Chellaboina, W.M. Haddad, D.S. Bernstein, D.A. Wilson. Induced convolution operator norms of linear dynamical systems. *Math. Control, Signals Syst.*, 13:2000,216-239.
[25] A. Cheng, K. Morris. Well-posedness of boundary control systems. *SIAM J. Control Optim.*, 42(4):2003,1244-1265.
[26] R. F. Curtain, H. Zwart. *An Introduction to Infinite-Dimensional Linear Systems Theory*. Vol. 21 of Texts in Applied Mathematics, Springer-Verlag, 1995 (1995).
[27] Munther A. Dahleh. Robust controller design: Minimizing peak-to-peak gain. 1992. *LIDS-P-2129*.
[28] M. A. Dahleh, J.B. Pearson. l^1-optimal feedback controllers for MIMO discrete-time systems. *IEEE Trans. Autom. Contr.*, AX-32, 1987.
[29] M. A. Dahleh, P.G. Voulgaris, L.S. Valavani. Optimal and robust controllers for periodic and multirate systems. *IEEE Trans. Autom. Control*, 37(1):1992,90-99.
[30] M. N. Dao, D. Noll, P. Apkarian. Robust eigenstructure clustering by nonsmooth optimization. *Int. J. Control*, 88(8):2015,1441-1455.
[31] M. N. Dao, D. Noll. Minimizing the memory of a system. *Mathematics of Control, Signals and Systems*, 27(1):2015,77-110.
[32] M. N. Dao, D. Noll. Simultaneous plant and controller optimization based on nonsmooth techniques. *Lecture Notes in Engineering and Computer Science. Proc. Word Congress Eng. Comp. Sci. (WCECS 2013)*, vol. II, pp. 855 - 861.
[33] C.A. Desoer, M. Vidyasagar. Feedback Systems: Input-Output Properties. *SIAM Classics in Applied Math.* 55, 1975.
[34] I.J. Diaz-Bobillo, M.A. Dahleh. Minimization of the maximum peak-to-peak gain: the general multiblock problem. *IEEE Transactions on Autom. Contr.*, 38(10):1993,1459-1482.
[35] J.C. Doyle, C. C. Chu. *Robust control of multivariable and large scale systems*. Honeywell Systems and Research center, AD-A175 058 final report, 1986, 188pp.
[36] K.-J. Engel, R. Nagel. *One-Parameter Semigroups for Linear Evolution Equations*. Springer Graduate Texts in Mathematics, Springer Verlag, 2000.
[37] H. Feichtinger. A novel mathematical approach to the theory of translation invariant linear systems. *Recent Applications of Harmonic Analysis to Function Spaces, Differential Equations, and Data Science*, Springer Verlag, pp. 483-516, 2017.
[38] M. Gabarrou, D. Alazard, D. Noll. Design of a flight control architecture using a nonconvex bundle method. *Math. Control, Signals and Systems*, 25(2):2013,257-290.
[39] P. Gahinet, P. Apkarian. Frequency-domain tuning of fixed-structure control systems. *IEEE Proceedings of 2012 UKACC International Conference on Control*, 2012, 178-183.
[40] E. Giner, J.-P. Penot. Subdifferentiation of integral functionals. *Math. Programming*, 168:2018, 401-431.
[41] A. Linnemann. Computing the L_1-norm of continuous-time linear systems. *SIAM J. Control Optim.*, 40(6):2007,2052-70.
[42] I.M.Y. Mareels, D.J. Hill. Monotone stability of non-linear feedback systems. *J. Math. Syst., Est. and Control*, 2(2):1992,275-291.
[43] T. Matsumoto, L.O. Chua, M. Komuro. The double scroll. *IEEE Trans. Circuits Systems*, 32(8):1985,797-818.
[44] A. Megretski, A. Rantzer. System analysis via integral quadratic constraints. *IEEE Trans. Autom. Contr.*, 42(6):1997,819-830.
[45] G. Meinsma. J-spectral factorization and equalizing vectors. *System and Control Letters*, 25:1995,243-249.
[46] F.A. Miranda-Villatoro, F. Forni, R.J. Sepulchre. Analysis of Lur'e dominant systems in the frequency domain. *Automatica* 98:2018,76-85.
[47] Anca Maria Nagy, Gilles Mourot, BenoÃőt Marx, Georges Schutz, JosÃĺ Ragot. Model structure simplification of a biological reactor. *15th IFAC Symposium on System Identification*, SYSIDâĂŹ09, Saint Malo, France, 2009.
[48] D. Noll. Cutting plane oracles for non-smooth trust-regions. *Pure and Applied Functional Analysis*, 5(3):2020,671-704.
[49] D. Noll. Second order differentiability of integral functionals on Sobolev spaces and L_2-spaces. *Journal für die reine und angewandte Mathematik*, 436:1993,1-17.
[50] D. Noll. Graphical methods in first and second order differentiability theory of integral functionals. *Journal of Set-Valued Analysis*, 2:1994, 241-258.
[51] S. Ohno, Y. Yoshimura. State space realizations robust to overloading for discrete-time LTI systems. *Signal Processing*, 156, march 2019, 12-20.

[52] L. Ravanbod-Shirazi, A. Besançon-Voda. Friction identification using the Karnopp model applied to an electromagnetic actuator. *Proc. Inst. Mech. Eng.*, 217(2):2003 part I: J. Systems and Control Engineering.
[53] R.M. Redheffer. On a certain linear fractional transformation. *J. Math. Phys.*, 39:1960,269-286.
[54] N.K. Rutland, P.G. Lane. Computing the 1-norm of the impulse response of linear time-invariant systems, *Systems and Control Letters*, 26(3):1995,211-221.
[55] C. Roman, D. Bresch-Pietri, C. Prieur, O. Sename. Robustness to in-domain viscous damping of a collocated boundary adaptive feedback law for an anti-damped boundary wave PDE. *IEEE Trans. Autom. Control*, 64(8):2019,3284-3299.
[56] B. Saldivar, S. Mondié, J. Loiseau, V. Rasvan. Suppressing axial-torsional vibrations in drillstrings. *Journal of Control Engineering and Applied Informatics,* SRAIT, 14:2013,3-10.
[57] B. Saldivar, S. Mondié, J.C. Ávila Vilchis. The control of drilling vibrations: a coupled PDE-ODE modeling approach. *Int. J. Appl. Math. Comp. Sci.*, 26(2):2016,335-349.
[58] P. J. Seiler. Stability analysis with dissipation inequalities and integral quadratic constraints. *IEEE Trans. Autom. Control.*, 60(6):2015, 1704-1709.
[59] P. J. Seiler, A. Packard, G.J. Balas. A dissipation inequality formulation for stability analysis of integral quadratic constraints. *IEEE Conference on Decision and Control*, 2010,2304-2309.
[60] A. M. Simões, P. Apkarian, D. Noll. A nonsmooth progress function algorithm for frequency shaping control design. *IET Control Theory and Appl.*, 2(4):2008,323-336.
[61] A. M. Simões, P. Apkarian, D. Noll. Nonsmooth multi-objective synthesis with applications. *Control Engineering Practice*, 17(11):2009,1338-1348.
[62] A. M. Simões, D. Alazard, P. Apkarian, D. Noll. Lateral flight control design for a highly flexible aircraft using nonsmooth optimization. *Aerospace Science and Technology*,15(4):2011,314-322.
[63] E. Sontag. From linear to nonlinear: some complexity comparisons. *Proc. IEEE CDC, New Orleans*, 1995, 2916-2920.
[64] N. Syazreen Ahmad, W.P. Heath, G. Li. LMI-based stability criteria for discrete-time Lur'e systems with monotonic, sector- and slope-restricted nonlinearities. *IEEE Trans. Aut. Contr.*,58(2):2013,459-465.
[65] M. Sznaier, F. Blanchini. Mixed L^1/H_∞ controllers for MIMO continuous-time systems. *Proc. 33rd CDC*, December 1994.
[66] A.R. Teel. On graphs, conic relations, and input-output stability of nonlinear feedback systems. *IEEE Trans. Autom. Contr.*, 41(5):1996,702-709.
[67] M. Unser. A note on BIBO-stability. `arXiv:2005.14428v2 [math.FA] 15 Sep 2020`, 10pp.
[68] J. Veenmann, C. Scherer. Stability analysis with integral quadratic constraints: A dissipativity based proof. *Proc. IEEE Conf. On Dec. Control*, Dec. 2013.
[69] M. Xia, P. Gahinet, N. Abroug, C. Buhr, E. Laroche. Sector bounds in stability analysis and control design. *Int. J. Rob. Nonlin. Control*, 30:2020,7857-7882.
[70] G. Zames. On the input-output stability of time-varying non-linear feedback systems. Part I: Conditions derived using concepts of loop gain, conicity, and positivity. *IEEE Trans. Autom. Control*, AC-11(2):1966,228-238.
[71] H. Zwart. Linearization and exponential stability. arXiv:1404.3475v1, 2014.
[72] Control System Toolbox 2020b, MathWorks, Natick, MA, 2020.